Alma Mater Studiorum – University of Bologna

SCHOOL OF SCIENCE
Department of Industrial Chemistry "Toso Montanari"

Second cycle degree in

Low Carbon Technologies and Sustainable Chemistry

Classe LM-71 - Scienze e Tecnologie della Chimica Industriale

Optimization and characterization of a wheat-based biocomposite for additive manufacturing

Experimental degree thesis

CANDIDATE

Erika Zamboni

SUPERVISOR

Chiar.mo Prof. Laura Mazzocchetti

CO-SUPERVISOR

Dott.ssa Paola Natali

Dott. Niccolò Giani

Dott. Stefano Scurti

Academic Year 2021-2022

Table of Contents

1. Introduction

Many innovations have been introduced in the last century, and polymers are one of the most significant. Since the ’60s plastic completely invaded the material’s market. In the previous years many materials with different applications and properties were synthetized for the first time, as polyvinyl alcohol (PVC), nylon, polyethylene terephthalate (PET), and polypropylene (PP). They were cheap, easy to use and to produce and very versatile. But there were some issues that the majority of the people did not care about: they derived from fossil sources, and they were not biodegradable or compostable. Neither they thought that some toxic substances could be present in some materials because there were no studies that confirmed that. Only later, when some researches had been performed, some substances contained in the plastics had been almost removed from the market (as BPA), and more attention is actually taken during the planning of the production.

But actually, the real question that should be asked is: which is the real problem, the plastic materials, or their utilisation?

When it is talked about plastic, it is generally referred to the waste island in the oceans, the fishes poisoning, the dirty in our cities, but not about the incredible innovations that they brought along. Cars are more efficient and safer thanks to the plastic utilised for their bodies, all the electronic devices are partly made of plastic improving their lightweight. Also airplanes, trains, and a lot of every-day life commodities have been improved by the utilisation of plastic.

So why is it still though that plastic should be avoided?

If it is put the focus on the real core of the problem, it is not the excessive use, because if it was completely recovered and reused the wastes would be around zero. The real target is the end of life.

The possibilities for the end of life of plastics are three: the recycling, the incineration, and the production of compostable materials. The first two options will certainly increase, but the first is not possible for all the materials, and the second requires a lot of energy (that usually is not produced by sustainable sources) and releases a large amount of CO_2 in the atmosphere. It is so essential to develop the last category, that is also the most recent and does not represent a large percentage in the overall end of life of the plastics, as represented in the *figure 1*.

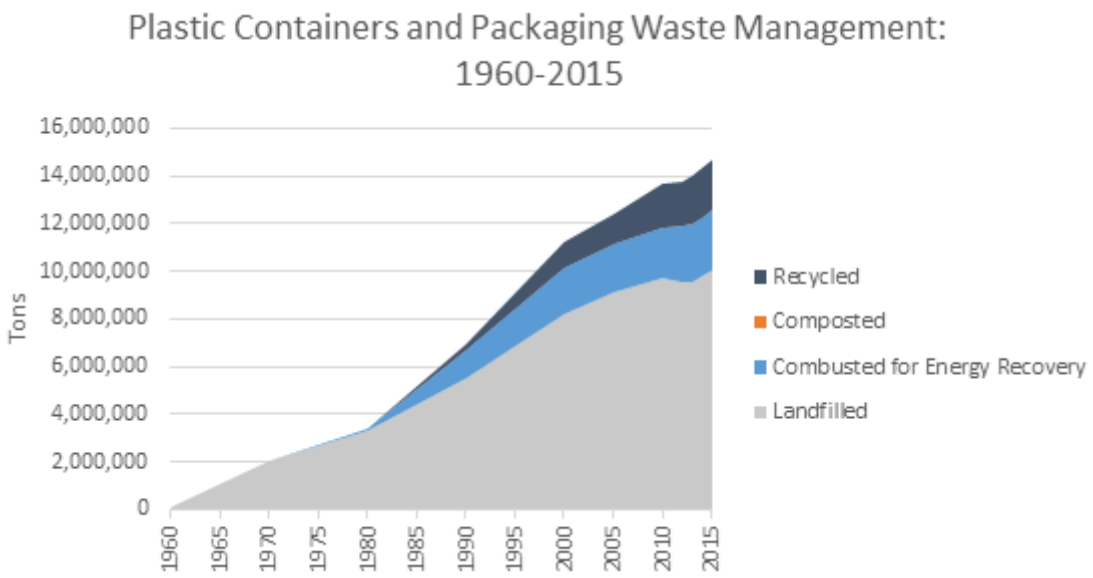

Figure 1 Graph of the plastic container and packaging waste management between 1960 and 2015

1.1. Bioplastics

Bioplastics are that category of materials that are biodegradable, biobased or both (European Bioplastics, 2016). It is first essential to make a distinction between "bio-based", "biodegradable" and "compostable" plastic. Biobased plastics are the ones synthetized starting from biomass instead of oil (Iwata, 2015). Biodegradable plastics are the ones that are recognized from enzymes already present in nature (Razza and Innocenti, 2012). The difference between biodegradable and compostable is that the first one can be degraded from microorganisms enzymes into carbon dioxide, water and methane without the releasing of toxic substances. The second one is completely degraded within a given and well-defined amount of time forming compost, a substance formed by microelements, active microorganisms and humus [2]. The latter is a complex mixture of organic compounds and acts as nutritional source for the vegetal organisms.

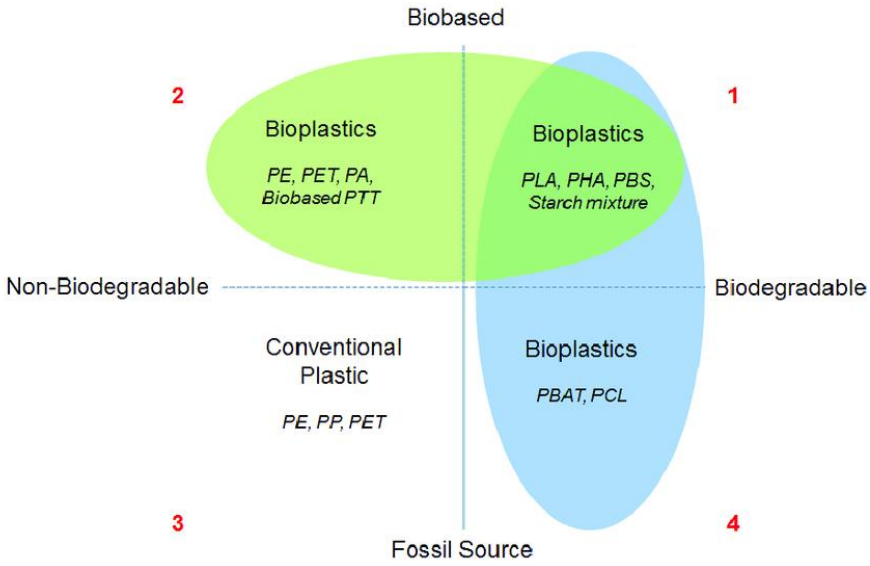

Figure 2 Coordinate system of bioplastics (European Bioplastics, 2011)

Biodegradable plastics can also derive from fossil raw materials, and it is not possible to define the origin of the final polymer from its chemical structure. The only method to distinguish the biobased and the fossil-based polymers is with a ^{14}C analysis, since in the first case the carbon atoms have not enough time to decay to ^{12}C so there is the coexistence of both the isotopes (new carbon), instead in the other one all the carbons are decayed to ^{12}C. It is possible to measure the Biobased Carbon Content (BCC) that is the fraction of new carbon over the total carbon present in the material, the result is a percentual value that represents the quantity of the material that derive from biomass. The parameters and the information related to the biobased content are contained in the International Standard ISO 16620 [3].

The plastic categories are represented in *figure 2*, where are represented in the vertical axis the origin of the material (biomass or fossil) and in the horizontal axis it is indicated the biodegradability. The most utilised commodities can be both biobased and fossil based as polyethylene (PE) and polyethylene terephthalate (PET). But they are not biodegradable, so it is necessary, especially for short-life commodities, to focus on the other part of the graph, in materials that are both biobased and biodegradable, as polylactic acid (PLA) and polyhydroxyalkanoates (PHA).

PHA are more difficult to produce since they are synthesized by gram-positive and gram-negative bacteria and are accumulated at intracellular level. Genetic manipulations are under study in order to increase the productivity of the bacteria. Depending on the manipulations and on the feeding of the bacteria, the polymer can be composed by macromolecules with different

side chains and can vary in their lengths. Last, an extraction is performed, in order to remove the polymer from the interior of the bacteria [4].

The PLA is instead easier to produce and to process.

1.1.1. Polylactic acid

Polylactic acid is a biobased and biodegradable polymer, produced starting from waste of biomasses as maize, potatoes and casava with biorefining processes.

The PLA is a very versatile and innovative material, for several reasons:

- it is synthetized starting from biomass, so the CO_2 released in the environment during the production and the disposal can be reutilized by the plants during the growth, for a carbon neutrality;
- it can be derived from wastes, so it can be non food-competitive;
- it is biocompatible, so can be utilized in medical applications;
- during its degradation it does not release toxic substances in the environment;
- it is easy to be processed, in the injection molding or in the additive manufacturing;
- it has some mechanical properties that are comparable to the ones of fossil-based commodities as polyethylene terephthalate (PET) [3].

Its monomeric unit is the lactic acid, that can be produced following different pathways.

First the monomer is produced starting from sugars as maltose and glucose, fermented by bacteria with the production of lactic acid, that is neutralized and purified. Also different chemical synthesis can be followed for its production, the main ones are the lactonitrile, acrylonitrile or propionic acid. They are less common, since they produce both the isomers of L-lactic acid (it will produce PLLA) and D-lactic acid (from which there will be the production of PDLA), this mixture is not suitable for all the applications, since the resulting polymer will not have any control over stereochemistry in the repeating units. Another con of these type of synthesis is that they are related to fossil-derived products (in this case the PLA is not biobased) and so there is the loss of the advantage to be independent by the market fluctuations, and they are more expensive [5].

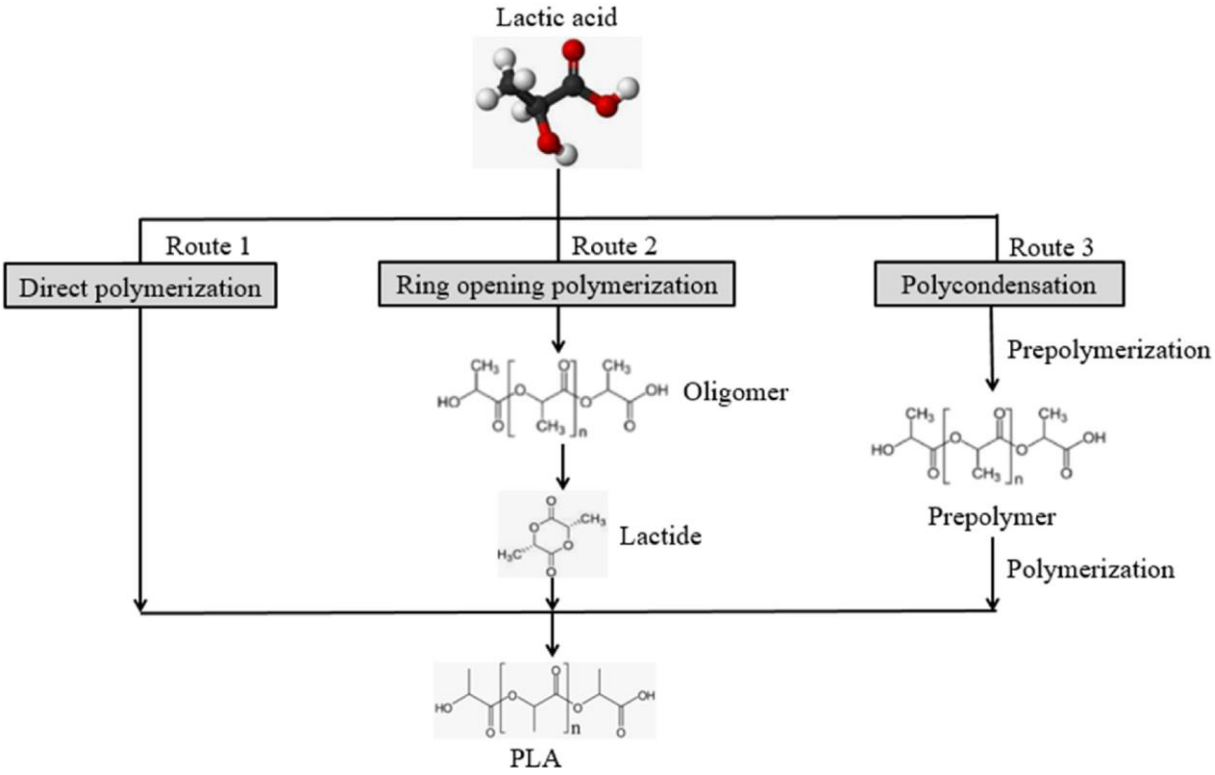

Figure 3 Pathways to produce the polylactic acid [5]

The lactic acid can polymerize following different pathways represented in *figure 3*, as ring-opening in lactides or self-condensation of the monomers, but the most common is the direct poly-condensation. The last method produces the PLA with the lower molecular weight, due to the impurities that can be present in the fermentation mixture and the requirement for removal of by products such as water that form along the process. The ring-opening method involves an internal transesterification with the formation of an oligomer that rearranges in a lactide ring first and then to the high molecular weight PLA. In the polycondensation method there is the addition of monomeric units, to form a high molecular weight oligomer, but side-reactions and byproducts can be present. For each of these pathways is usually required a catalyst [6].

After the production, when requirements are fulfilled, PLA can crystallize. The crystalline domain represents the area of the polymer in which the macromolecules are ordered, it is required a determined delay and temperature to give the energy and the time to the macromolecule to be able to rearrange in this type of structure. It influences the properties of the polymer, as hardness, stiffness, modulus and tensile strength [7]. The degree of crystallinity defines different final applications of the polymers depending on it being amorphous or semicrystalline, as their glass transition and melting temperature can significantly vary and modify the overall polymer behaviour.

The PLA presents some issues during the crystallization, since it requires a very large amount of time at quite high temperature; in order to save energy usually some nucleating agents are utilized, mostly of inorganic origin as carbon nanotubes or mica [8]. It can develop different crystal phases, α, β and γ. They have some differences in the arrangement, but are based on a helix, disposed in different conformations depending on the temperature and the mechanical stresses that were applied on the material during the production [9].

The PLA properties are related to its degree of crystallization and to its molecular weight, the higher they are, the higher is the time required for its biodegradation, that can take years [9]. This can be a positive property since, depending on the type of utilization, the material can be projected to have a shorter (for short-life commodities) or longer (for long-life products) degradation time. The tensile strength and the elastic modulus are similar to the ones of PET, but it has poor toughness, so its elongation at break is very low (less than 10%). Side chains along the main backbone are not present, for this reason the macromolecules are not reactive and require surface treatments if some chemical modifications are required [10].

The PLA applications are very large:

- biomedical (for its biocompatibility): in surgery, prosthetic and drug-delivery systems, since the material can be projected to degrade in a certain amount of time and do not release toxic substances in human body;
- packaging, since they can be composted at the end of their life together with food scraps;
- films, since PLA is impermeable to oxygen and can protect food without damaging it.

But further studies are actually carried out, that imply other applications [9].

Some studies were performed on the degradability of the PLA materials and on the effects of the ageing. In particular a study on a PLA-hemp fibre biocomposite conducted by M.S. Islam, K.L. Pickering and N.J. Foreman [11] showed, after 1000 h of ageing, a decrease in the coefficient of thermal expansion, due to the exposure to UV light, an increase in the weight of the samples due to the adsorption of water (since PLA, in the amorphous regions, can be hygroscopic). Also the mechanical properties dropped, as the tensile strength and the Young modulus, mainly related to the swelling stresses inside the samples caused by the absorption of water. The crystalline domains do not absorb water, since the macromolecules are very densely packed one to each other, while the amorphous regions can withdraw moisture. For this reason, the degradation is faster in the PLA with lower degree of crystallinity.

Typically a higher degree of crystallinity decrease the speed of degradation. With a high temperature hydrolysis the macromolecules are shortened, and bacteria enzymes are able to disrupt them. For this reason, disposable products should be formed by PLA with lower molecular weight and anyway treated in industrial plants were temperature control can be applied to speed up the process [12].

Except the biodegradation in natural environment the other pathways that a material could take at its end-of-life are the incineration and the recycling. The incineration can be a good option, since there will be the recovery of the energy utilized in the production of the material, and the CO_2 released would follow the carbon neutrality pathway as it was previously said. The recycling presents some issues, since the PLA is not a long-life material, and it would be extremely difficult to utilize it twice, for the reasons related to the ageing.

1.2. Composite materials

Polymers are very versatile materials since it is possible to modify some of their characteristics to make them fit a particular need. It was previously said that some attention can be put during the production phase, as in the case of PLA the crystallization rate can influence the final properties, but there is another method with almost unlimited possibilities: the mixing of the polymer with other components, forming a composite material.

A composite material is formed by two or more materials and have improved properties with respect to the single components. Composites are mainly composed by two parts:

1. the matrix, which constitute the major part presents in the final material and provides cohesion linking the fibers of the filler, it gives the shape of the material and provides the chemical resistance. It can be a thermoplastic, thermosetting or elastomeric polymer;
2. the reinforcement, that is responsible for the change in some mechanical properties. It is usually a material with higher tensile strength and rigidity than the matrix, and it is added to reinforce the material. It is usually an elongated particle or a continuous fibre, as glass fibres. A filler can be utilized as reinforcement, it is an inert material that change the properties of the matrix (mechanical, electrical or thermal) or reduce the price of the final composite. It must be compatible with the basis resin and must have high wettability. The most commons are organic (as cellulose, vegetable fibers and starches), but can be also mineral (as silica, talcs and alumina) [13].

Other components can be present, as:

3. the additives, that change the properties of the material during the processing or in the final use, and are related to some main actions as plasticizers, stabilizers and lubricants [13];
4. the compatibilizer, whose action is related to the interaction between the filler and the matrix. When the components are incompatible this material is added to suppress their phase separation and to increase the interactions between the two components. It does not provide further properties but increase the homogeneity between the phases in the composite [14].

The final product is heterogeneous, characterized by a continuous phase (the matrix) interspersed by discontinuous phases (the reinforcement). The composites can be of three main types, depending on the origin of the matrix: organic, mineral or metallic [13].

Figure 4 Example of a biocomposite composed by a bio-resin and wood wastes

Biocomposites represent the category of composite materials in which the filler is composed by natural components and the matrix is also potentially sustainable (some examples are represented in *figure 4*). They present some benefits with respect to the synthetic fillers, as the low cost, since they usually derive from wastes, the carbon neutrality of the filler at their end-of-life, and they are widely available. The most utilized are based on cellulose or on lignin, extracted from biomasses as hemp, flax, sisal, banana, wheat and rice. Depending on the source of the material, on the area and on the age, the filler can have different characteristics and properties, but they are generally lightweight. The origin and the type of material define the

applications that it can have, actually they can be utilized in different sectors, as automotive, building, construction, prosthetics and storage tanks [15].

The miscibility of the matrix and the reinforcement, during the formation of the composite, follows the Flory-Huggins equation, represented in the equation (1).

$$\Delta G_m = kTV\left[\frac{\varphi_1}{V_1} ln\varphi_1 + \frac{\varphi_2}{V_2} ln\varphi_2\right] + \varphi_1\varphi_2\chi_{12}kTV/v_r \quad (1)$$

Where V is the total volume, V_i is the molecular volume of component i, φ_i is the volume fraction of component i, k is the Boltzman's constant, χ_{12} is the Flory-Huggins interaction parameter and υ_r is the interacting segment volume [19].

This equation demonstrates the decrease in the miscibility of solvent-polymer mixtures with respect to solvent-solvent mixtures, it is related to the decrease of the combinatorial entropy of mixing.

When temperatures or solvents are changed in the environment of two miscible polymers two processes can occur: the nucleation and growth or the spinodal decomposition. The first one can occur also in the metastable region and not only in the unstable one, and is related to the growth of a separating phase around a nucleus. The second one is related to the spontaneous decomposition of a single phase into two distinct phases. As it is possible to see from the graph in *figure 5*, there is a strong dependence of the temperature on the miscibility and the stability of the blend (mixture of two or more polymers). Two areas at the top and at the bottom of the graph are present, that represent the regions in which the polymer is immiscible. When a copolymer is produced it must respect the temperatures defined by its phase diagram, or there will be a phase separation. This graph can be modified with some chemical manipulations, as the addition of a compatibilizer (an additional polymer), or the treatment of the surface of the polymers, in order to make them more reactive and decrease the interphase energy. [19]

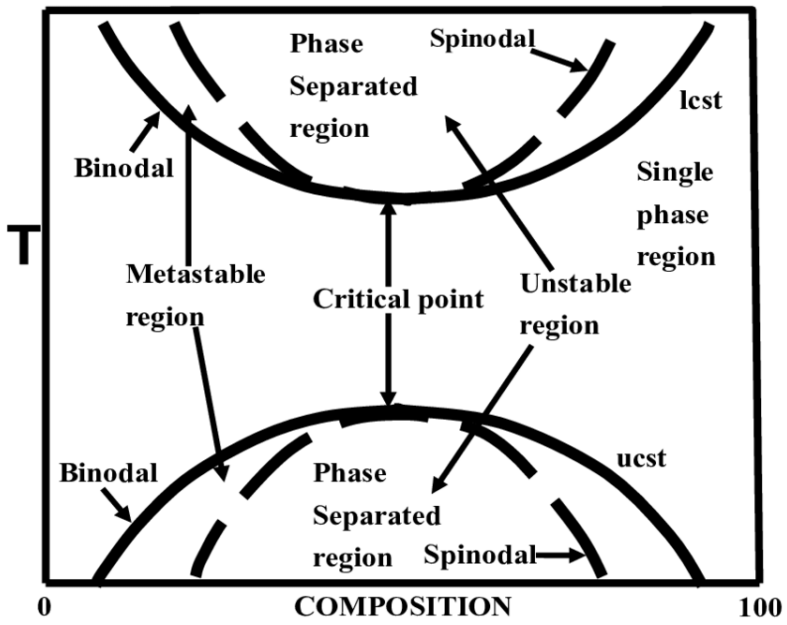

Figure 5 Diagram of a binary mixture of two polymers as a function of temperature. Lcst is lower critical solution temperature and ucst is upper critical solution temperature.

1.2.1. Compatibilizer

The biocomposites have many potentialities but can present some issues related to the anisotropy of the material that can be enhanced when the filler and the matrix are not interacting with each other. In this case there is the formation of an interphase, an area in which the surface of the matrix and the filler are separated, and this creates a weakness in the material.

In order to overcome this issue, a reactive molecule can be utilized, that acts as a bridge between the macromolecules of the matrix and the ones of the filler, forming chemical bonds. In this way the interlayer is minimized, since the molecules of compatibilizer reduce and occupy it, and the material is overall strengthened for the decrease of the anisotropy and the increased interaction between all the components of the composite [14].

In the biocomposites field, mostly when it is related to cellulose, compatibilizers are very common. The most utilized are polymers grafted with maleic anhydride, it increased the interfacial adhesion, it generally shows an increase in elastic modulus but not in toughness [16]. The other issue of maleic anhydride is that it is fossil based, for this reason it is not suitable by a sustainable point of view.

In order to synthetize a new compatibilizer, it should follow the 12 principles of green chemistry, or at least the majority of them. They were written in 1998 by Paul T. Anastas and by John C. Warner:

1. Prevention: to prevent the production of wastes is better than reclaim them;
2. Atom economy: the materials utilized should be incorporated in the final product in the largest amount that is possible;
3. Less hazard: utilize and produce materials with the lower grade of toxicity for humans and the environment;
4. Safer chemicals: the efficacy of the reagents should remain high while the toxicity is decreased;
5. Safer solvents: to utilize the lower amount of solvents that it is possible, or make them innocuous;
6. Energy efficiency: if it is possible, the reactions should be conducted at ambient temperature and pressure;
7. Renewable feedstocks: utilize renewable raw materials each time that it is possible;
8. Reduce derivatives: try to avoid the derivatization;
9. Smart catalysis: utilize catalyst to improve the reaction rate and speed;
10. Degradable design: at the end-of-life the product should be degradable in order to not persist in the environment;
11. Real-time analysis for pollution prevention: continuous control to check if some hazardous materials are formed;
12. Hazard and accident prevention: the materials and methods utilized should be the ones with the lower risk for chemical accidents, as releases, explosions and fires [17].

For these reasons, biobased components are more suitable.

Xyloglucan is a polysaccharide extracted from the seeds of the tamarind tree, which function is to physically link cellulose microfibrils. A study of A. Marais et al. [18] in which xyloglucan are mixed with the PLA to produce a composite materials was performed, in which the PLA is polymerized along the surface of the compatibilizer via ring-opening polymerization. From the study it was possible to conclude that the compatibilization was correctly performed, but there were some issues related to the moisture absorption that decreased the length of the PLA chain during processing owing to transesterification.

Another option could imply the utilization of a more common material: the polyvinyl alcohol (PVA). It is synthetized starting from the polymerization of the vinyl acetate, that forms the polyvinyl acetate, which is then hydrolysed in order to remove the acetate group and to obtain the polyvinyl alcohol (chemical structure represented in *figure 6*) [20].

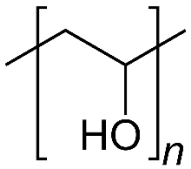

Figure 6 Chemical structure of the polyvinyl alcohol (PVA)

It is a biopolymer and soluble in water, biocompatible, biodegradable (require 6-12 weeks to completely degrade) and nontoxic, it has high mechanical properties, but has a high price. Its properties are related to the molecular weight, that range generally between 10000 and 400000 MW, but also to the percentage of hydrolysis, as it is represented in *figure 7* [20].

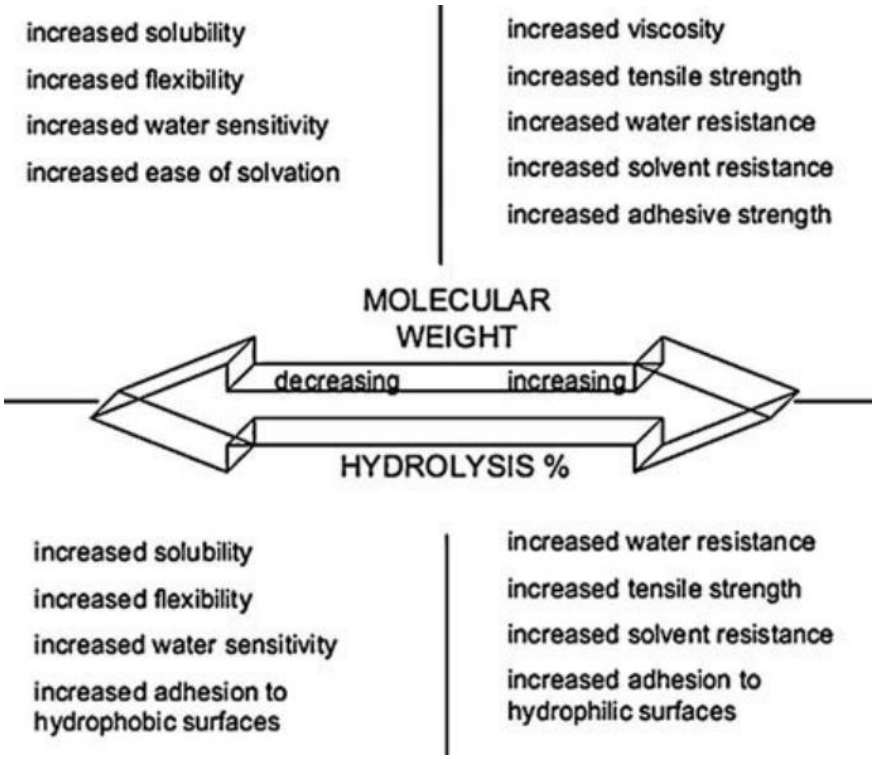

Figure 7 Schematic representation in the change of the properties of the PVA depending on its molecular weight and its % of hydrolysis

It is a semicrystalline polymer, and sometimes a plasticizer is recommended, in order to reduce the degree of crystallinity in bulk, to increase its processability and flexibility and to decrease

its melting temperature and brittleness. It is also highly hydrophilic, so it is necessary to pay attention to the moisture content, that can decrease the mechanical performance.

It is highly compatible with polymers as starch, cellulose and lignocellulose, but also with other polymers as PLA, since a blend of these two polymers show a single T_g peak. It can be utilized in packaging, but its applications are generally in blends of polymers. [20]

Some modifications can be performed on the PVA, as the addition of reactive moieties that increase its reactivity. As it was previously said maleic anhydride is a common option but, since it is not suitable for a biopolymer, other molecules should be considered, as levulinic acid.

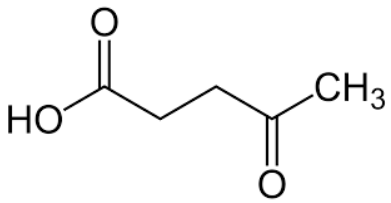

Figure 8 Chemical structure of levulinic acid

Levulinic acid is a short-chain fatty acid (as represented in *figure 8*) and since it has a carboxylic and a carbonylic group it is very reactive to many types of derivatives. It can be synthesized form many raw materials, as 5-hydroxymethyl furfural, furfural, polysaccharides, starch and lignocellulosic wastes. The last ones are the most promising ones and the most utilized, since they are cheaper and widely available, but they present some issues since are more inert. For this reason, a pre-treatment is necessary to free the hexose sugars that they contain, that can be mechanical, chemical, physical, physicochemical or biological. Depending on the complexity of the lignocellulosic part present in the raw material the pre-treatment can be different. The cellulosic and hemicellulosic parts require a less effective treatment. Once the hexose sugars are free they can be treated in different ways, but the most common is the biorefining process. It comprises two acid-catalysed steps, first to convert the sugars into hydroxymethyl furfural, that is then hydrolysed to levulinic acid with a yield of 70-80 mol%, and the coproduction of formic acid [21].

It can be utilized as fuel, in pharmaceuticals (in cancer and tuberculosis therapy), as food additive, but also as functionalizing agents in polymer composites.

1.2.2. Biofiller

As it was previously said, an important component of the composites is the reinforcement, the component that increases the strength and provide peculiar properties to the final material. It can change the melting, crystallization or glass transition temperatures, can increase or decrease the hydrophilicity, the biodegradability, the flexibility, the elongation at break, the elastic modulus, the processability, the weight, or reduce the price or the environmental impact related to the production of the material. For these reasons the composite materials are very versatile, depending on the components that are added to the matrix they can fit a large variety of applications.

The biofiller are that particular category of reinforcement that derive from biomass, usually from food wastes (third generation resources) since they are cheap and abundant, but can derive also from primary/secondary generation resources such as cotton, flax, hemp or wood [22].

These raw materials are formed by plant cells, composed by three main parts (as it is represented in *figure 9*):

- the lignin, constitute for the major part the secondary cell walls, and it represents 10-25% of the total dry matter. It is not crystalline, and it contains many different aromatic compounds. It acts as crosslinker between the sugars presents in cellulose and hemicellulose, conferring the mechanical strength and the hydrophobic characteristic to the cell wall. Its function is to transport water and nutrients. It requires very long and difficult extraction processes in order to obtain the single molecules, for this reason it is not very utilized and further studies need to be implemented to exploit this resource;
- the hemicellulose, it accounts for the 20-40% of the overall plant cell-wall polysaccharides. It is a shorter chain polysaccharide (500-3000 sugars unit) composed by a large variety of sugars, as glucose, xylose, mannose, galactose, rhamnose and arabinose. It is not a crystalline polymer but it is amorphous with little strength. Its function is to control the cell enlargement, it links adjacent cellulose supramolecular aggregates and prevents them to separate;
- the cellulose, it is the most abundant biopolymer in the biosphere, composed by glucose units linked by a β-1,4 glycoside bond, responsible for the flatness of the ribbon of the molecule (stabilized by hydrogen bonds) and the structural ability to pack together in a very tight manner. It is a crystalline polymer since the simplicity of the chemical structure allows it to create very ordered domains. For these reasons, for its particular

properties and since it is easier to extract (even if it generally implies the utilization of harmful substances, and this is not coherent with the green chemistry principles), it is widely utilized as biofiller. [3]

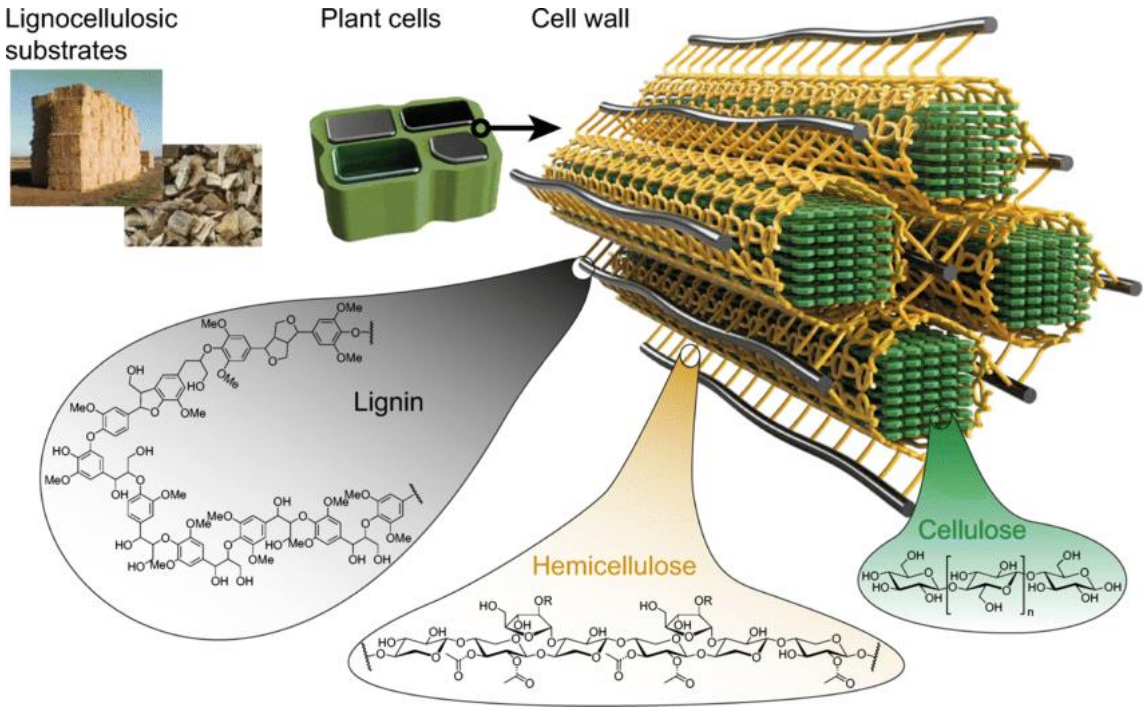

Figure 9 Schematic representation of the structure of a plant cell constituent

Cellulose is extracted with different methods, as chemical, mechanical, alkali, boiling and retting, but the latter is the more common [25].

Cellulose has many properties, as quite high thermal resistance (its glass transition temperature is between 220-250 °C and the decomposition temperature is higher than 200°C so it decomposes before becoming flexible hence, does not behave as thermoplastic), it is insoluble in common organic solvents and in water, even if it is hydrophilic. The -OH groups are disposed mainly on the inside of the macromolecules, involved in a complex network of hydrogen bonds, and this make cellulose less reactive. For this reason and to improve surface roughness, usually surface treatments are utilized. They also favour the interaction between the polymer and the fiber, increasing the mechanical strength of the biocomposites. It exists a large amount of surface treatments, as ultrasonic treatment, steam explosion, silane treatment, alkali treatment, isocyanate treatment, benzoylation, mercerization, acetylation, latex coatings, peroxide and enzymatic treatment. The alkali treatment is the most common, cheaper and easier to perform [26].

Alkali treatment is based on water and on NaOH. First the samples are conditioned at 65% relative humidity at 20°C for 48 hours, then they pass into four compartments: the alkali treatment (with a concentration of NaOH between 2.50-3.30 M), the stabilization treatment (in which the concentration of NaOH was 20% of the initial one), the washing (utilizing water at 80°C) and the neutralization (using acetic acid 80% v/v). This treatment modifies the properties of cellulose, changing the crystallinity, pore structure, accessibility, stiffness, but also mechanical and chemical properties as dimensional stability, tensile strength and reactivity. It is easier to perform this type of treatment on cellulose with lower degree of crystallinity, since the molecules of sodium hydroxide find more difficulties to enter in more compact and ordered regions, instead the amorphous ones presents some voids in which the molecules can enter more easily [27].

Cellulose is subjected to many modifications, the most common ones are with ether and ester (as the acetate), in order to change its properties but, as in the case of cellulose acetate, the substitution make the polymer more difficult to biodegrade.

PLA-cellulose biocomposites were widely studied. In a particular study conducted by A. Awal, M. Rana and M. Sain [28] it was utilized a particular additive that worked as compatibilizer to improve the interaction between the filler and the matrix, since PLA is hydrophobic while cellulose is hydrophilic. The study showed an improvement in the processability of the material, an increase in the tensile modulus of 26% compared to the single PLA, but this effect was not present in the case of the PLA-cellulose without the compatibilizer. This proved that the two materials do not interact strongly one with the other, for this reason an additive is required.

Other biocomposites were studied, as the one discussed by P. Toro, R. Quijada, M. Yazdani-Pedram, J. L. Ariascd [23], in which the material was composed by Eggshell and polypropylene. It showed an increase in the tensile modulus and elastic modulus with respect to the one formed by polypropylene and calcium carbonate (from talc). Another study performed by A. A. Hussein, A. A. Sultan and Q. A. Matoq [24] showed that a biocomposite composed by low density polyethylene (LDPE) and shrimp shells had improved mechanical properties as tensile strength, young modulus, stress at break and stress at yield with respect to the single polymer.

An innovative method, to further increase the sustainability of the production of the biocomposites materials, is the additive manufacturing, even if it is not suitable for all type of materials. The most common ones are the composites of PLA, since it is highly processable in instruments as the 3D printer.

1.3. Additive manufacturing

The additive manufacturing is a recent and innovative technology based on the addition of layers of materials forming a 3D network. It is completely different from the other methods of production, which are based on subtractive or forming manufacturing. The subtractive method consists in the subtraction of materials from a block in order to create a sample with a particular shape. It is highly expensive, mostly for the high amount of wastes that are created. The forming manufacturing is instead based on the melting of a material that will fit a particular mould, and will be subjected to stresses as compression, shear and tension. The issue related to this method is not the difficulty in producing different shapes, but the lack of flexibility in the production, since to accommodate changes in the shape it is necessary to change the mould, that is the most expensive component in the process, and a certain amount of wastes is nonetheless produced [29].

Additive manufacturing requires lower spaces, the amount of wastes is almost zero (it depends on whether the sample that is produced require supports to be created, in this case the amount of wastes increase), it can be utilized with multi-materials, the instrument do not require specific parts depending on the nature of the material that is extruded and complex structures and shapes can be produced [29].

The most common technologies of additive manufacturing are the stereography SLA, the Digital Light Processing (DLP), the Selective Laser Sintering (SLS) and the Fused Deposition Modeling (FDM). All of them require that the sample that must be printed is first designed with a software of Computer-Aided Design (CAD), that will produce a file that will be read by a slicer that will convert it into a format (G-code) that can be elaborated by the instrument.

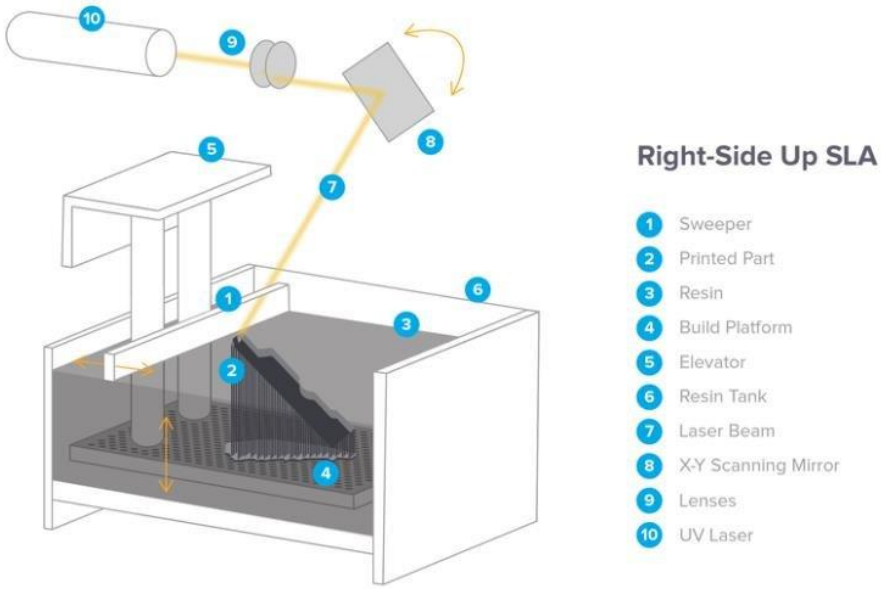

Figure 10 Schematic representation of a SLA instrument

The DLP and the SLA utilize liquid precursors, contained inside a vat. It is irradiated UV light, that permit the resin precursors to crosslink forming a layer, the platform will go down and another layer will be formed above the first one (as it is represented in the *figure 10*). The main difference is that the DLP irradiates an area to cover the whole section of the object, instead the SLA covers only a single portion with the irradiating source that has to move around the surface to cover the path to be hardened [31].

The SLS is instead a method that is utilized for metals, in industrial plants. It utilizes metal powder, that is locally melted by a high power laser [30].

The last method is the FDM, it is the most versatile, easier and more commercialized.

1.3.1 Fused Deposition Modeling

The FDM is also known as Fused Filament Fabrication (FFF), Modeling Extrusion (ME), Fused Layer Manufacturing (FLM) or 3D printing. The instrument can be customized depending on the needs of the company, but it is generally composed by some main parts which are represented in *figure 11*:

- the chamber of extrusion, into which the filament is inserted and melted;
- the nozzle, from which the molten filament exits;
- the bed, above which the nozzle passes depositing a 2D layer of the molten filament.

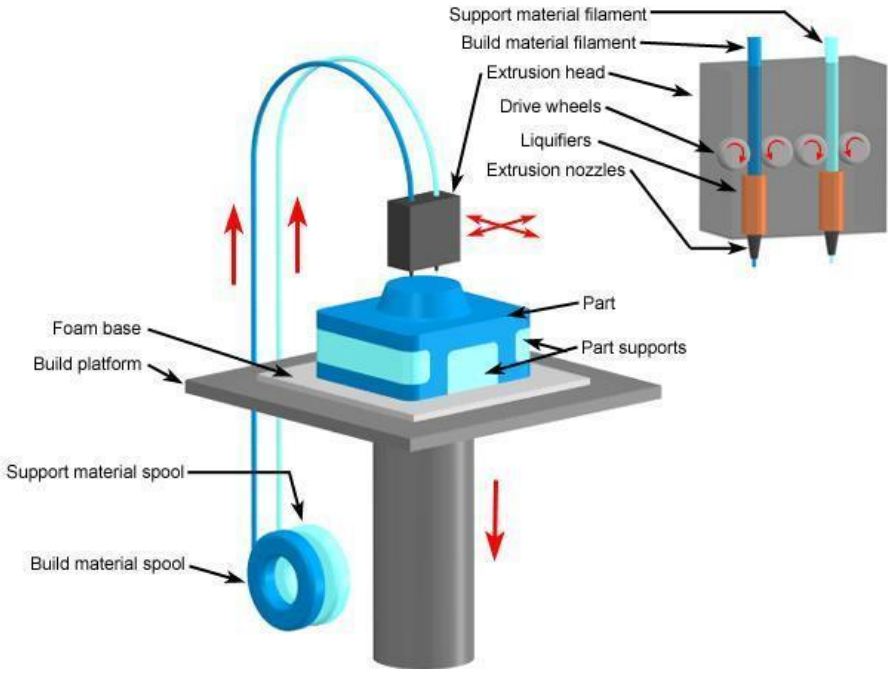

Figure 11 Schematic representation of a 3D printer

Depending on the type of instrument two nozzles can be present, in order to have the possibility to print with two different materials. Above the nozzle it is present a thermocouple, that read and adjust the temperature of the extruder and of the nozzle, depending on the parameters set by the slicer. The bed can be heated, which is particularly useful with materials in which warping can occur (it is the shrinkage of the material, in which the borders of the polymer detach from the bed and create a curved object, it can occur in some materials that are sensible to the difference in temperature between the upper and the lower layers) [32].

The slicer is the software that defines the conditions that the 3D printer must follow during the production of the sample designed with a CAD software. Inside this program many parameters are defined, as the diameter of the nozzle and of the filament, the temperatures, the speed of extrusion (generally are defined different speeds for the outlines, usually the lower one since it is required more precision, for the first layer, because the adhesion with the bed should be improved, and for the infill, to decrease the time required to produce the object) and of the nozzle and the supports if they are required. It is generally first created a contour, its thickness can be decided defining the number of contour layers, that will be filled up by the infill. It can be decided the percentage of the infill of the object (so the density of the volume of the final object that will be occupied by the extruded material, it is a value comprised between 0-100%), the layer thickness and its geometry that can follow a concentric, rectilinear, grid or honeycomb

(hexagonal) pattern. Other types of geometry can be utilized, but they are less common and specific for particular applications, as represented in *figure 12* [33].

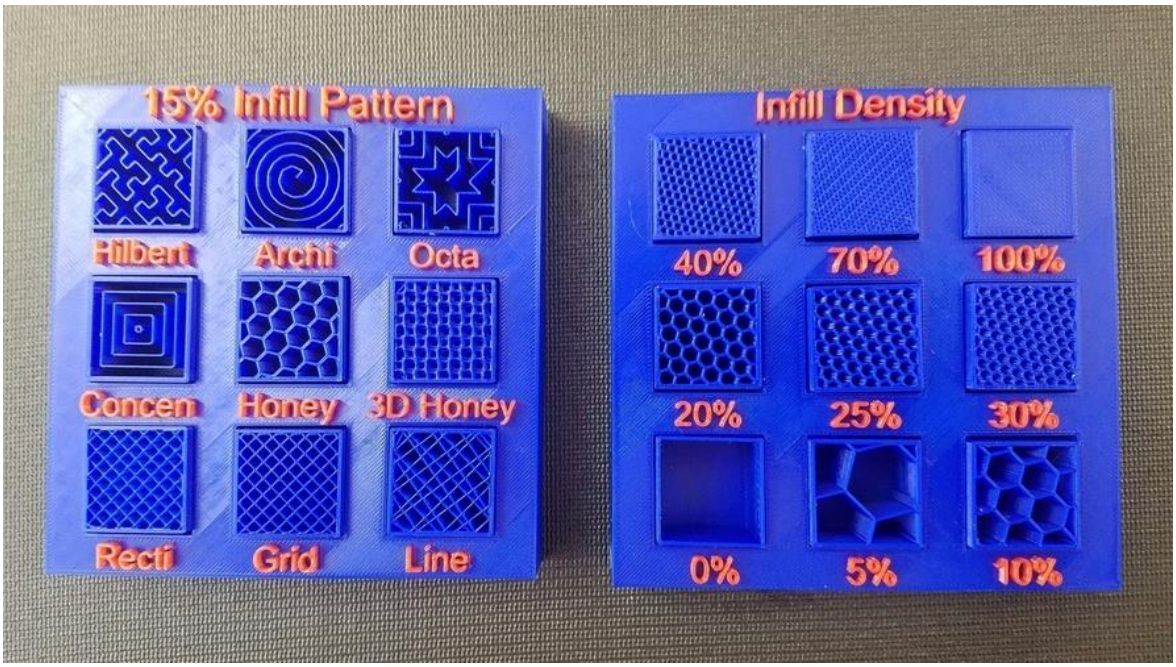

Figure 12 Representation of the pattern and density of the 3D printing

The nozzle moves along the X and Y axis, in order to create the layers of the object, and on the Z axis in order to develop the object, creating new layers above the bottom ones.

Also the printing direction should be considered, because there will be differences in the mechanical properties. It is related to two main orientations, as it is represented in *figure 13*:

- the build direction, that can be along the X axis (on the edge), along the Y axis (flat) or on the Z axis (upright). Generally, the higher mechanical properties are present in samples printed along the X axis;
- the angle of deposition, that is generally a value of 0°, 45°, 90° or 135° (in the *figure 13* are represented the samples obtained with an angle of 0° and of 90°). There are differences in the mechanical properties, that are higher when the stress is applied along the same direction of the deposition angle [33].

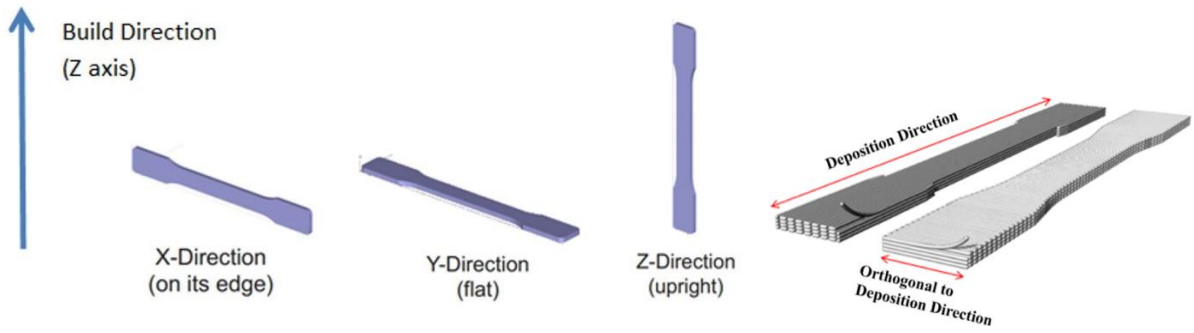

Figure 13 Representation of the build direction (on the left) and of the angle of deposition (on the right), at 0° and at 90°

One of the issues in the 3D printing technology is the weakness of the interlayer bonds. For this reason, if a stress is applied along the printing direction, the material shows higher mechanical performances, if instead it is applied perpendicularly to the printing direction there will be a direct involvement of the interlayers, that are weaker, and the material will have decreased mechanical properties. The build direction instead shows improved values when it is along the X axis because the base on which the object is developed is larger, and the deposition of the layers is more stable [33].

There are other issues in the utilization of the FDM technology other than the interlayer strength, as the possible presence of voids, due to a temporary modification of the extrusion flow, the difficulties in the optimization of the printing parameters, since there are many different variables that influence the final product, the possibility of develop toxic vapours when certain materials are utilized: however, being a new technology, the studies and the resolution to problems are still under development [30].

It is however worth to point out that there are also a large amount of pros, as the low space that is required for the equipment, the lower amount of wastes produced that can be converted into an economic advantage, the substitution of the material is easy, specific parts depending on the polymer that is extruded or on the object that it is created are not required. The materials that are generally utilized do not produce toxic vapours (as PLA), it can be created an infinite number of shapes for the objects that can be rapidly tailored when needed. The application sectors are wide, but it is mostly involved in the biomedical and aerospace areas, as well in prototyping and for small volume productions. [30]

Different polymers can be utilized for the 3D printing, the most commons are:

- Acrylonitrile butadiene styrene (ABS): it is a thermoplastic and amorphous polymer. It is a copolymer composed by the three polymers that compose its name. It is fossil-based, and it is not biodegradable, but it has improved impact resistance and toughness, and it is also resistant to abrasion. It is resistant to chemicals and thermally stable, it has low thermal expansion coefficient (so the object that are created are dimensionally stable). Its melting point is 230°C, suitable for the extruder of the 3D printer, and can warp, so a heatbed is required. It emits toxic vapours during the extrusion;
- PLA: a thermoplastic polymer, biodegradable and with a melting temperature between 170-180°C (so it is required less energy with respect to other polymers) that depends on the degree of crystallinity of the material. It has high tensile strength and it is easy to print, since it does not warp and so a heatbed is not required. To improve its properties a large amount of (bio)composites of PLA are studied;
- Polycarbonates (PCs): they present high strength, durability and toughness, but their melting temperature is higher than other polymers;
- Polyether ether ketone (PEEK): thermoplastic semicrystalline polymer with good heat resistance, mechanical properties and chemical stability, but it has high melting temperature (>350°C). Due to this very high temperature the 3D printers could face some damages and special equipments should be implemented; moreover, there are issues as delamination since the lower layers have very low temperatures with respect to the upper ones during deposition. It is utilized in medical field since it is biocompatible, but it is more expensive than other thermoplastic polymers.
- Polyetherimide (PEI): it has high strength to weight, but has high extrusion temperature, and it needs a heatbed since warping can occur.
- Nylon: it has high toughness and impact resistance but can absorb water (decreasing the mechanical properties) and can warp [33] [34].

Other materials can be utilized, but they are less common.

Among all the materials previously reported, the most interesting one is the PLA, by a sustainable point of view, because it is the most common for the home 3D printer and it is the simpler to utilize, it does not emit toxic vapours during the extrusion, it has low melting temperature and it does not require a heatbed.

1.3.2. 3D printing of PLA and of PLA biocomposites

As it was said in the previous paragraph, PLA is one of the most interesting polymer for the 3D printing. It is generally a transparent filament (as it is represented in *figure 14*), but it can have different colours depending if some fillers or additives are added.

Figure 14 PLA pure filament with an object created with the FDM technology

Different studies have been performed, one in particularly conducted by L. Fontana et al. [35], is focused on the layer thickness, the infill percentage and the moisture absorption (since as it was said in the chapter 1.1.1. Polylactic acid is a polymer that can adsorb a large quantity of water, and this decreases the mechanical properties). The first two variables influence the properties of the final material, but if they are too high a larger amount of material is utilized, and the time for the production increases, so the energy required and the overall process is more expensive. For these reasons it is necessary to find a balance. They discovered that keeping the printed samples at room temperature and at 50% humidity did not affect the ultimate tensile strength (UTS), and that the optimal layer height is 0.15 mm and the optimal infill is 50%. The other printing parameters were: temperature of 215°C, travel speed along x-y directions of 150 mm/s, along the z direction of 23 mm/s, infill print speed of 90 mm/s, first layer print speed of 30 mm/s and speed for outlines of 20 mm/s.

Another study, conducted by M. M. Hanon, J. Dobos and L. Zsidai [36], was focused on the mechanical properties of printed PLA depending on the direction of printing, on the orientation and on the layer height. The orientation along the X axis favoured an increase in the Young modulus, of the ultimate tensile strength and of the hardness, instead the elongation at ultimate tensile strength and at break are higher in the orientation along the Y axis. The direction of the deposition angle influenced the mechanical properties, showing a decrease of them in the case

of 45° angle deposition withing the gauge length and 0° of the other region. There was an increase in ultimate tensile strength, elongation at UTS and at break with the samples with a layer thickness of 0.1 mm, but the Young's modulus increased with the specimens with layers of 0.2 mm thickness. The fracture profile was clean, an showed the geometry utilized during the printing. Generally the orientation was the most impacting factor, showing higher mechanical properties for the printing along the X axis (on the edge).

It is necessary to specify that these studies (as they explain themselves) cannot be considered completely applicable to any other case, since there are some parameters, as the 3D printer utilized and its biases, the filament of PLA utilized that may presents some defects and can have different degree of crystallinity. They should be considered as a general overview on which it is possible to formulate basic idea about its own project.

Other studies have been performed on PLA biocomposites, in order to decrease the overall cost of the final product, to change some specific properties of the material and to improve its processability. As it was said in the chapter 1.2.2. Biofiller, in the case of utilization of cellulose (that is the most widely utilized) it is recommended the use of a compatibilizer in addition to a surface treatment in order to improve the adhesion between the matrix and the filler, to decrease the energy of the interphase between them. It is important also to consider the degradation temperature of the reinforcement, since if it is higher than the temperature set for the extrusion the material will degrade.

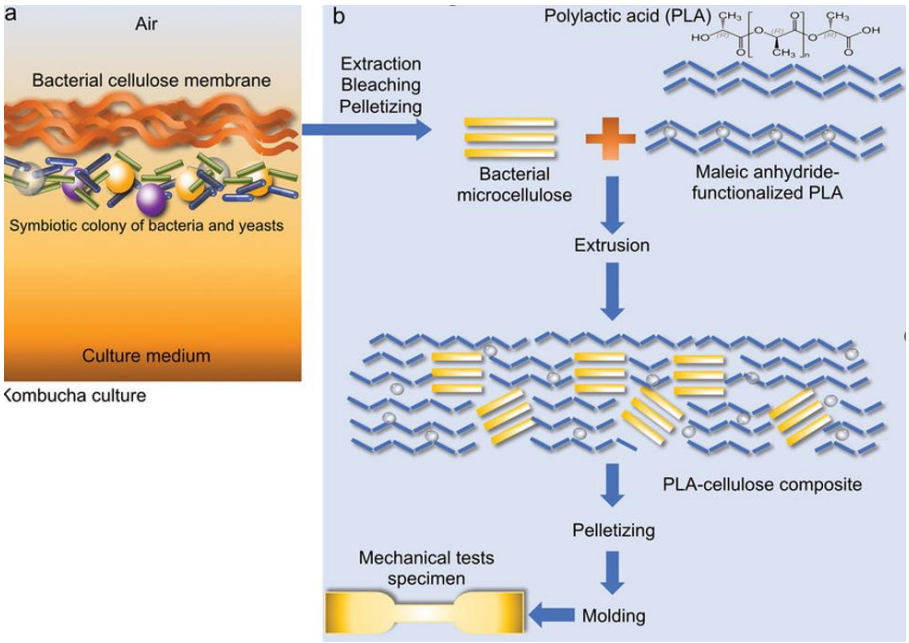

Figure 15 Chemical structure of PLA-cellulose biocomposites with the addition of a PLA-g-MA compatibilizer [38]

In *figure 15* it is represented an example of production of a biocomposites specimen starting from bacterial cellulose (cellulose that is produced by bacteria). It is extruded as filament with the PLA (the matrix) and the PLA-g-MA (the compatibilizer, composed by PLA grafted to maleic anhydride that increases the chemical interactions) and then it is printed with a 3D printer, forming a specimen for mechanical test with a dog-bone shape. The use of the compatibilizer increases the mechanical properties, but decreases the sustainability of the material since maleic anhydride has fossil origin [38].

A very comprehensive review was performed by S. Bhagia et al. [37], considering the PLA as matrix and different types of biofiller, as cellulose, hemicellulose, lignin, rice husk, fruit pomaces and starch. They require some treatments in order to be utilized, since they must be of the correct size in order to homogenize as much as possible with the matrix and to not block the nozzle and they must be subjected to a surface treatment. They must be dry, since both the matrix and these type of biofiller absorb moisture that could create some voids during the extrusion and decrease the mechanical properties. The addition of an amount of biomass too large in the filament can create some issues as flow inconsistencies and diameter variations, that interfere with the printing quality. After a surface treatment, also the utilization of a compatibilizer is suggested, mixed with the biocomposites during the first extrusion of the material in order to create the filament or by melt blending. It was seen that in a large number of case the mechanical properties were improved.

In the study it was also compared the injection molding of some biocomposites materials with the 3D printing, which generally showed a decrease in the mechanical properties utilizing the FDM technology. This is related to the presence of layers, that represents a weakness in the material [37].

Their applications comprehend interiors buildings (if they are not exposed to sunlight or moisture that could degrade them), but it is generally utilized for packaging and short life objects. They are biocompatible, for this reason they can be utilized in medicine, ad some studies in the utilization of them in automotive sector are currently performed.

The recycling of these polymers is possible, collecting, washing, drying, sorting and shredding in order to extrude a new filament. But since these materials are sensible to moisture, UV light, they have not long life since they are generally biodegradable and increasing the number of extrusion can lead to a degradation of the material, the recycled filaments will have a strong decrease in the mechanical properties. For this reason, generally is preferred the composting (if

the material is compostable) in industrial plants, that is performed in a controlled environment and with specific conditions, and so is faster than home composting. It is performed in two months at 50-60°C, but can be improved with some chemical treatments that decrease the degree of crystallinity of the biocomposite. [39]

2. Purpose of the thesis

In recent years the anthropogenic pollution is a theme more and more discussed. The Anthropocene is the historical period in which the nature is completely altered by the human activity. The main related problems are well known, and a cause of them is the increasing quantity of plastic that is accumulating around the world, hence a change in the utilisation of disposable commodities is necessary. In 2015 it was estimated that the overall production of primary (derived from virgin materials) and secondary (recycled) plastic wastes reached 8300 Mt (between 1950 and 2015). Around 800 Mt of plastics had been incinerated and 600 Mt have been recycled, only 10% of which had been recycled more than once. Around 4900 Mt were discarded and are accumulating in landfills or in the natural environment [40]. This clearly define that it is necessary to change the fate of the wastes, so not to be left in the environment, but recycled, or increasing the utilization of biodegradable materials or, as last method, incinerated.

The recycling of plastics is promising, but need to be improved, since only a few types of plastic can be positively fully processed. There are issues in the recovery of the materials (since it's not always easy to separate the recyclable and non-recyclable plastics) and the recycling is difficult since the materials usually do not maintain the original properties, so need to be integrated with virgin materials. The incineration instead emits a large amount of CO_2 in the atmosphere, but can be a method to produce thermal energy, and to not introduce the materials in the environment creating further problems. Instead, the utilisation of biodegradable plastics could be a very promising innovation. The main problem related to them is that they usually derive from agricultural crops, so there is a competition with food. The technologies for their production are new and need to be implemented to reduce their productive costs. These are some of the main reasons why further studies on biodegradable polymers are needed.

The purpose of this thesis is related to the utilisation of biodegradable materials, in particular of PLA. The issue related to this polymer is the higher cost compared to fossil-based material, because fossil materials as PP, PE and HIPS cost between 1,50-2,67 €/kg in 2022 [41], while the cost of PLA is between 2-6 €/kg depending on the type of PLA present on the market [42]. Hence in the present work, to decrease the overall cost of the final material, PLA was modified by addition of a filler derived from agri-food wastes (wheat waste), that has presently no market options, and whose fate is animal feed. This is a good option since there is no food competition and it is a material with almost zero commercial value. Previous attempts at introducing such a

waste in PLA in different amounts and further processing in a filmat for 3D printing, showed in the final 3D printed items a decrease in mechanical properties [43, 44], so in the current project a different approach to maintain the characteristics of the PLA, for which it can be competitive with other fossil-based materials, has been evaluated.

The focus is thus on the application of a compatibilizer based on levulinic acid, to keep at the highest the biobased characteristic of the matrix, and poly(vinyl alcohol) that was synthetized on purpose. The utilisation of a compatibilizer should improve the interaction between the filler and the matrix, in this way the mechanical properties should not decrease.

The new compatibilizer obtained was first characterized with different methods, than was added to PLA and extruded as filament and printed with a 3D printer to create samples to be testes. The characterization (both of the single components and of the final filament) was performed with the utilisation of an AT-IR to check the real composition and if the synthesis was correctly carried out, a TGA to check the temperature and weight losses, a DSC in which we find out the glass transition temperature (T_g), crystallization temperature (T_c) and to see if there are some different arrangement in the polymeric structure with the increasing temperature. An NMR was performed on the compatibilizer to check the functionalization rate. To test the mechanical and thermal resistance of the material it was performed a traction test with a dynamometer and some dynamo-mechanical analysis (DMA).

A further attempt to evaluate the effect of the wheat waste to the modified PLA was finally carried out, with the aim to obtain a filament for 3D printing of the biocomposite.

3. RESULTS AND DISCUSSION

3.1. Synthesis of the PVA-g-LA

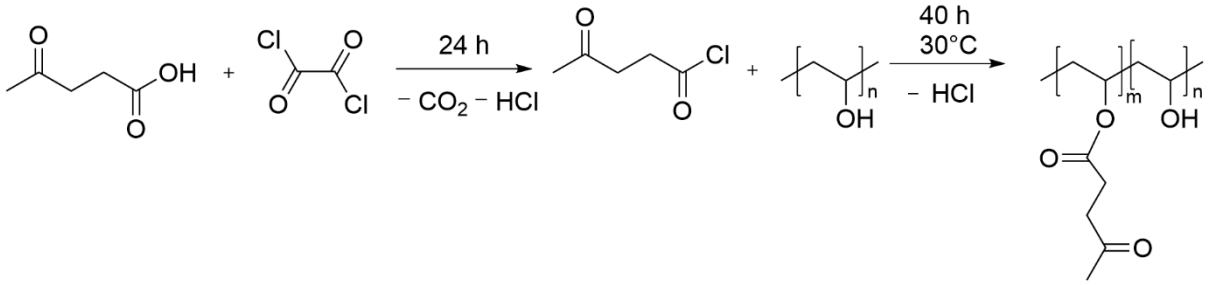

Figure 16 Scheme of the synthesis

The synthesis of the PVA-g-LA (schematically represented in *figure 16*) was carried out in a three-necked flask of 500 ml, placed under nitrogen atmosphere, in which 80 ml of levulinic acid (LA) and 2 ml of dimethylformamide (DMF) were added. After cooling the solution in an ice bath, 60 ml of oxalyl chloride dissolved in 200 ml of dichloromethane were dropped slowly into the mixture. At the end the ice bath was removed and the reaction was stirred for 24 hours (the *figure 17A* represents the batch of reaction). During the adding of chlorinated agent the solution slowly started to turn toward the yellowish. After 24 hours the mixture was transferred in a 250 ml flask and the solvent evaporated.

In next step 15 g of PVA were added directly to the chlorinated levulinate with molar ratio of 1:2 between PVA:LA. The reaction was kept under nitrogen atmosphere and stirred for 40 hours at 30°C. Then, the mixture was cooled down to room temperature and poured in ethyl ether. The precipitated polymer was washed with ethyl ether. During the evaporation of the ether, the powder turned from the initial greyish to the final orange, as it can be seen in the *figure 17B*. The final product was characterized by Nuclear Magnetic Resonance (NMR), Infrared spectroscopy (IR), Thermogravimetric Analysis (TGA) and Differential Scanning Calorimetry (DSC). The functionalization rate of the copolymer is 71%.

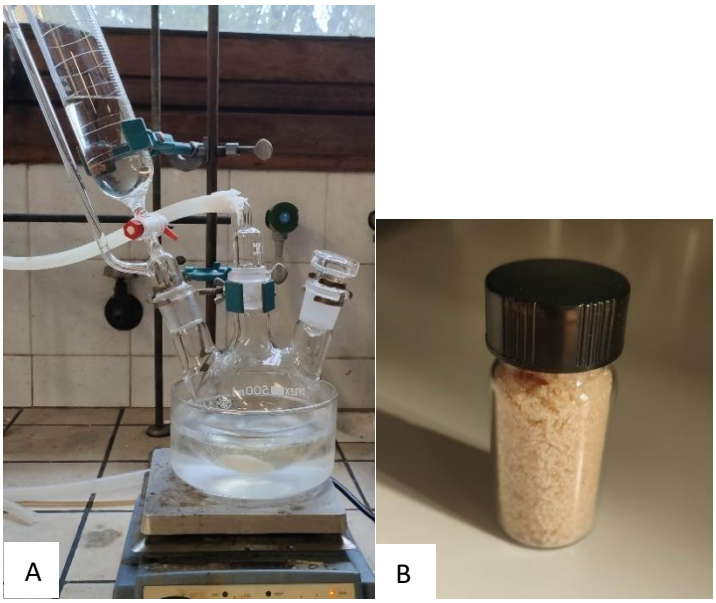

Figure 17 (A) picture of the first part of the synthesis; (B) picture of the final product

3.1.1. Characterization of the PVA-g-LA

Two main categories of analysis were performed: spectroscopic and thermic.

Different spectroscopic techniques were performed, the ATR FT-IR analysis was carried out to characterize the molecular structure of the synthetized compound and an NMR analysis was performed to estimate its functionalization rate.

The thermal analysis were performed by TGA to check the degradation temperature and the mass loss of the components of the PVA-g-LA and by DSC to check the glass transition temperature and the melting temperature.

3.1.2. Spectroscopic characterization

By FT-IR spectroscopy, the intermediate of the synthesis has been analysed in order to evaluate the correct functionalization. In *figure 18* the spectrum related to the product of chlorination of the levulinic acid is reported. In the Figure, the O-H stretch at 3000 cm^{-1} derived from the carboxylic acid clearly disappeared upon reaction.

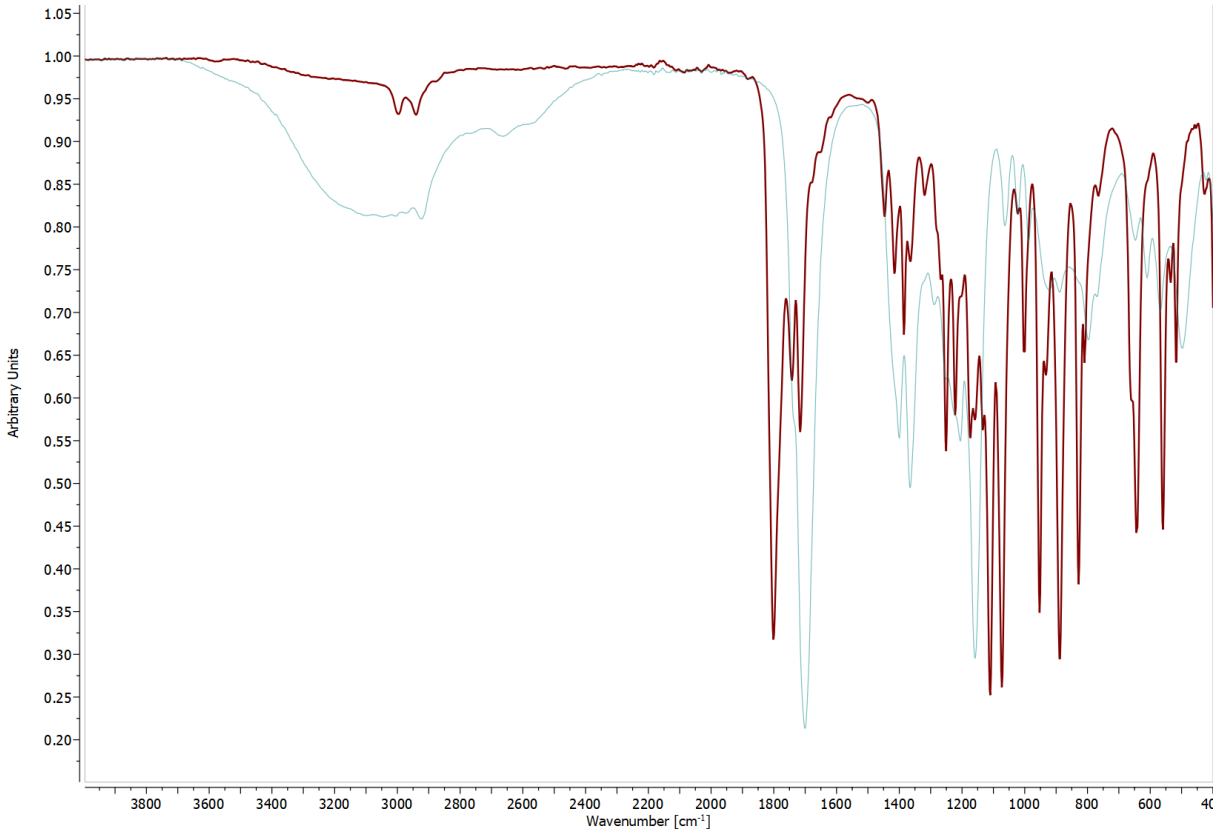

Figure 18 Comparison between the IR spectra of levulinic acid (blue line) and chlorinated levulinic acid (red line)

At the same time, the carbonyl absorbance peak was shifted from 1700 cm^{-1} to 1800 cm^{-1} confirming the formation of the chlorinated product. It is possible to conclude that the first intermediate was effectively obtained.

In *figure 19* the overlapped spectra related to the final product (PVA-g-LA) and the starting polymer (PVA) were reported.

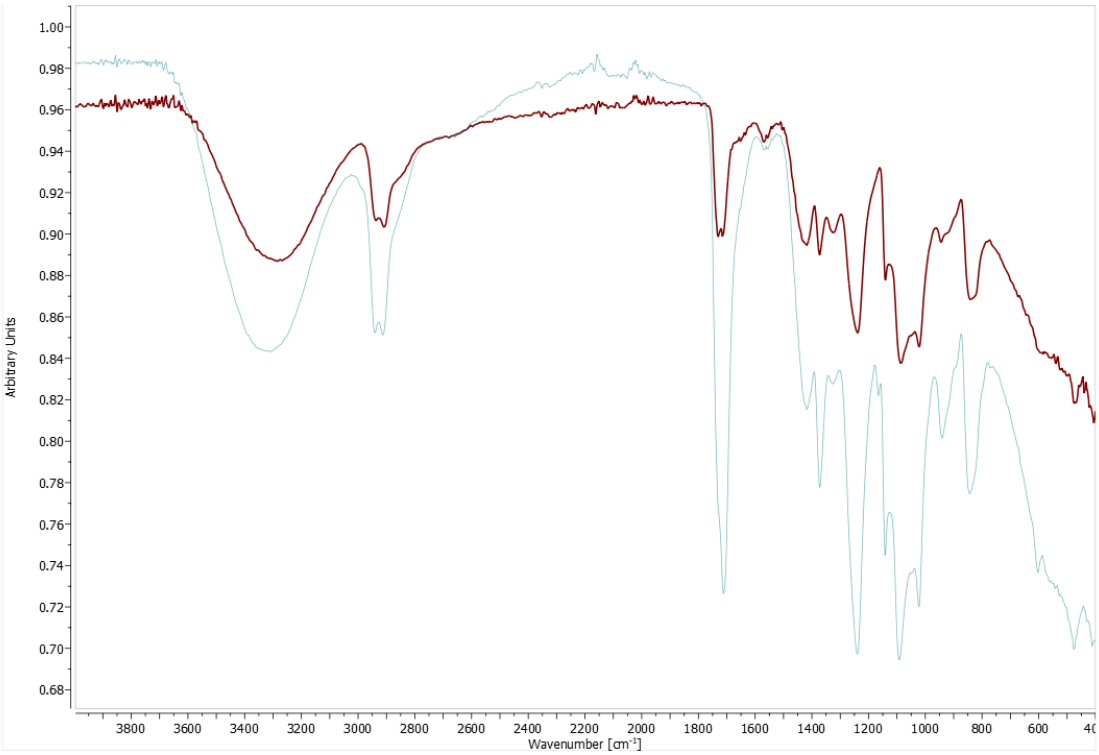

Figure 19 Comparison between the IR spectra of PVA (red line) and compatibilizer (light blue line)

There is an increase in the intensity of the carboxylic peak (1700 cm^{-1}) that is related to the functionalization and the creation of the ester bond with the levulinic acid. Such an observation suggests that the target molecule was obtained and that the synthesis was correctly carried out.

In *figure 20* the ^{1}H-NMR of the compatibilizer is reported, showing in the range between 2 -1 ppm the signals of the terminal methyl -CH_3 of the levulinic acid, the -CH_2 groups present along the chain of the levulinic acid as well as the -CH_2 related to the PVA backbone (A_2). At 3,8 ppm there is the signal of the -CH group of the PVA (A_1).

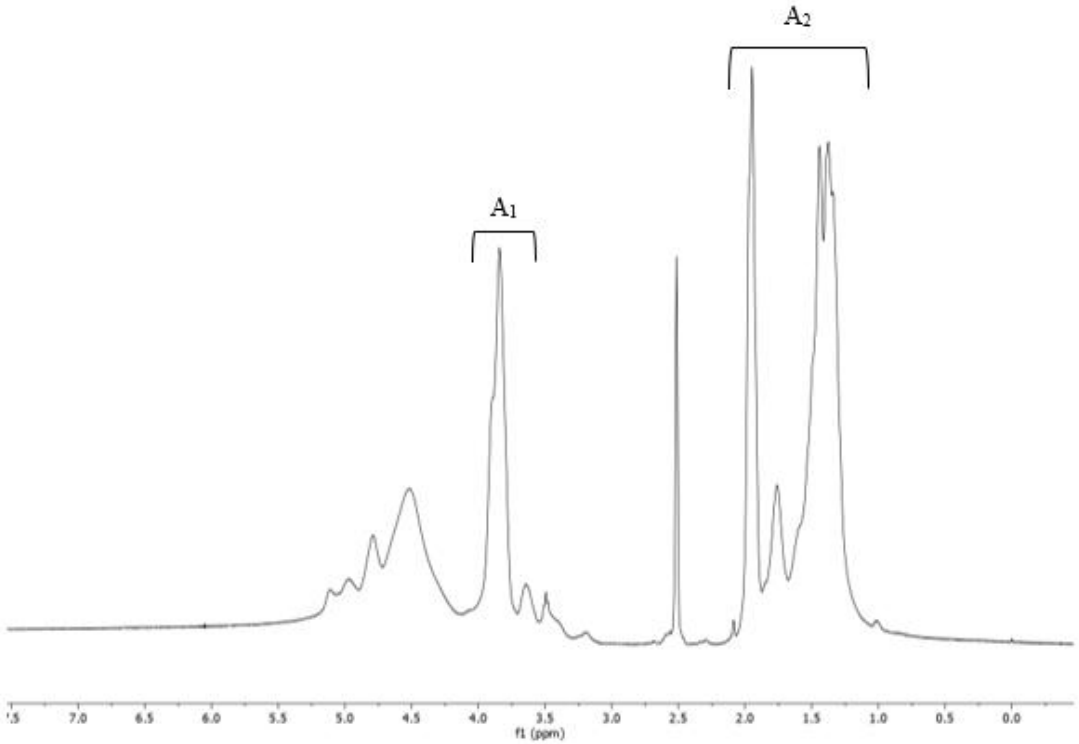

Figure 20 NMR spectra of the compatibilizer PVA-g-LA

To evaluate quantitatively the degree of functionalization and therefore the copolymer composition, the signals previously defined as A_1 and A_2 were properly integrated and by the following equation (2) it was evaluated the functionalization rate:

$$\frac{A_1}{\frac{A_1}{m_1}+\frac{A_2}{m_2}} \cdot 100 = \%\ \text{copolymer} \qquad (2)$$

where A refers to the area and m represents the number of protons involved.

The values of the integral of the two areas are 21,05 for A_1 and 78,95 for A_2, m_1 is composed by 1 proton (since only one is present in the CH group) and m_2 is composed by 9 protons (3 from the $-CH_3$ and 6 from the three $-CH_2$), so the result of the formula for the calculation of the functionalization rate of the copolymer (2) is 70.58%.

The synthesis was correctly performed and the functionalization rate is significant.

3.1.3 Thermal characterization

A Thermogravimetric Analysis (TGA) was also carried out in order to check the degradation temperatures (hence the thermal stability) and the relative mass losses that occurred in the material, the thermogram is represented in *figure 21*. A Differential Scanning Calorimetry

(DSC) measurement was carried out in order to define the transitions that occurred in the material as the glass transition, the possible crystallization and the melting with their relative temperatures and enthalpies.

The following thermogram in *figure 21* is related to the TGA analysis of the compatibilizer carried out in nitrogen atmosphere.

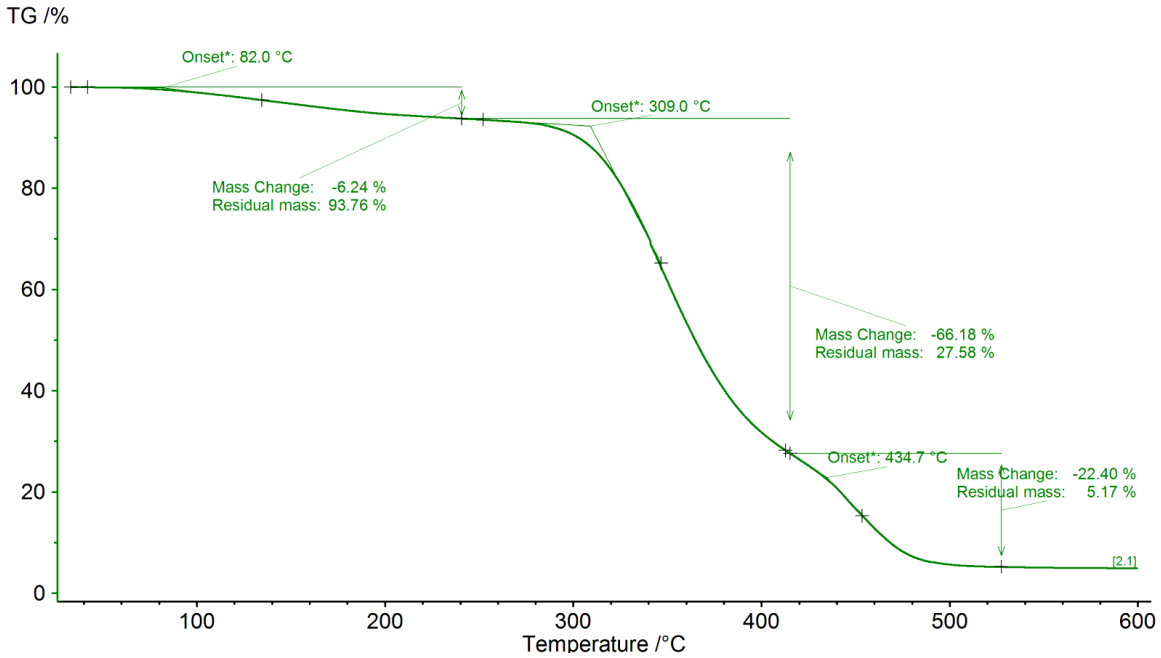

Figure 21 TGA thermogram of the compatibilizer PVA-g-LA

The first step of mass loss of 6% occurs around 82°C, it is related to the solvent remained inside the compatibilizer and to water evaporation. Then the major mass loss occurs at 309°C with a reduction of 66% related to the levulinic acid and to the PVA. Despite the pure reference materials (levulinic acid and PVOH) have degradation temperature around 245°C and 230°C respectively, in the thermogram the weight loss is nevertheless shifted at higher temperature owing to the new obtained structure of the macromolecule after the substitution and the formation of the copolymer. At the end of the analysis only 5% in mass remained, so almost all the material has been degraded and completely volatilized. What remained is the charred fraction from the macromolecule that was not volatilized under inert conditions.

The following thermogram in *figure 22* is related to the DSC analysis of the compatibilizer.

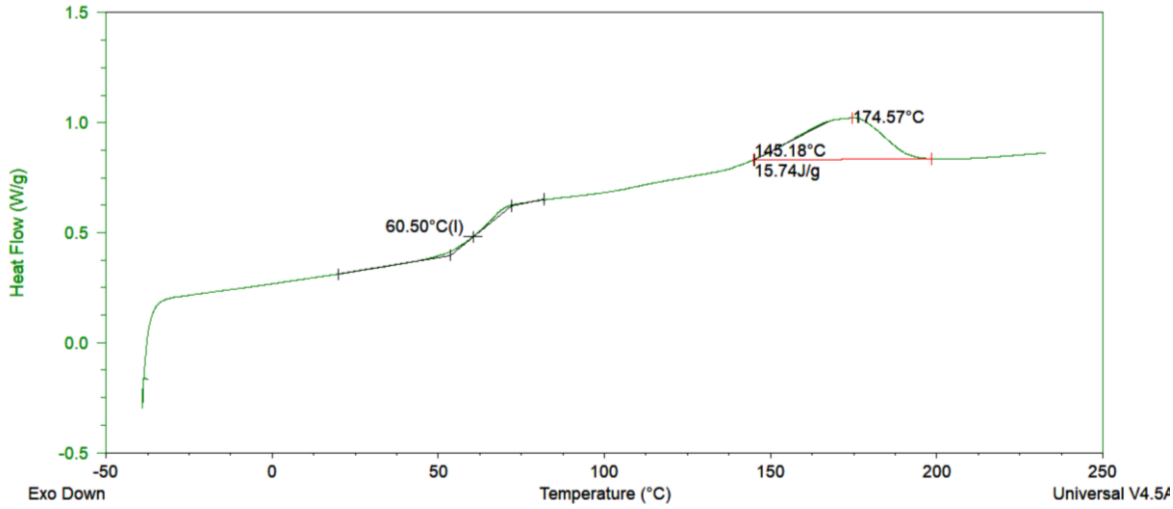

Figure 22 DSC thermogram of the compatibilizer PVA-g-LA

DSC thermogram showed the glass transition (T_g at around 60 °C) and the melting (T_m at 175 °C with a ΔH_m of 16 J/g) of the compatibilizer. There are no exothermic peaks and it is not present a crystallization peak. This is related to the chemistry of the PVA, since it is prevalently amorphous the small fraction that was able to crystallize is already in the crystal state and for this reason it is not present an exothermic peak in the thermogram.

3.2. Production of the filaments

Once the compatibilizer was successfully obtained, it was used first in blend with PLA to evaluate if the mixture could be extruded and could provide a valuable mechanical performance. A first mixing was carried out in a twin screw extruder, then the filaments were produced with a single screw extruder equipped with a dimeter feedback control in order to obtain a constant and stable filament that could be used for further 3D printing.

Some parameters can be set by the operator such as: the temperatures of the four different areas of the screw, the speed of the screw, the intensity of the cooling fans and the diameter of the filament. The latter was set at 1.75 mm (standard) and the cooling fans was set at 40% of the power, since at higher values the cooling was too fast and the macromolecules had very low time to rearrange in an ordered structure. The other parameters changed depending on the material extruded. Initially a 10% weight fraction of compatibilizer was added in the PLA matrix, obtaining a product labelled as PLA-C. Different amounts of compatibilizer were attempted (as in the list below) to be added to the PLA matrix, to which it was further added a 10% weight fraction of wheat middling for the biocomposite production, labelled as PLA-C-F.

For the sake of comparison also a sample with only the biofiller, labelled as PLA-F was produced.

Overall six filaments were produced. They are reported below with the compositions of the materials, all expressed by weight:

- PLA
- PLA-C with concentrations of 90:10
- PLA-F with concentration of 90:10
- PLA-C-F with concentrations of 80:10:10
- PLA-C-F with concentrations of 85:5:10
- PLA-C-F with concentrations of 88:2:10

The PLA, the wheat middling and the compatibilizer are all highly hygroscopic (the PVA present inside the compatibilizer tends to absorb water), the water absorbed could interfere with the extrusion (either creating voids upon evaporation or hydrolysing the polyester macromolecular backbone). Water can interact also with the levulinic side moieties, cleaving the ester bonds and releasing the pendant group. To decrease the moisture content, all the materials utilized for the extrusion had been dried in a furnace for 1 hour and half at 105°C, at a temperature that, based on the TGA of the compatibilized, should be safe for all the components involved.

Each filament was extruded two times, in order to increase the homogeneity (except the PLA, since homogenization was not necessary). After the first extrusion, a manual pelletization was performed, creating pellets long approximately 7 mm that were extruded a second time. The issue related to this step is to not degrade the material, since it is subjected to double heating at high temperatures. The spectroscopic and thermal characterizations, the ATR FT-IR, the DSC and the TGA, were also performed in order to assess that this did not occur.

The diameter of the filaments produced was however not constant, ranging from 1.50 mm to 1.90 mm. This can be related to the differences in length of the pellets, so to an inconstant feed to the screw of the extruder, to the presence of some voids caused by some residues along the screw that did not permit to the material to proceed, or to an imprecision of the instrument.

The filaments were different in colors and presented different diameters, and in *table 3* the diameter, obtained as mean value obtained from three measurements of the filaments with a digital calibre, is reported. This value is important, since it defines the suitability of the material

to be 3D printed. Then an observation on the colour of the filaments was performed, in order to recognize their main differences and see how the addition of some components changed the physical appearance of the filler.

Table 1 Physical description of the filaments

Material	Color	Diameter
PLA	Transparent	1.73 ± 0.20
PLA-C	White	1.68 ± 0.14
PLA-F	Brown	1.72 ± 0.02
PLA-C2-F10	Brown	1.40 ± 0.72
PLA-C5-F10	Brown	1.30 ± 1.05
PLA-C10-F10	Brown	1.52 ±1.17

The color of the matrix is transparent, since additives are not present and the crystallinity is low. An increase in the crystallinity would make the material opaque. The compatibilizer, that was first orange in color, mixed with the PLA gives rise to the white color of the filament. Instead the filler is brown in color, and it influences the final coloration of the filament. The three PLA-C-F have both the influence of the compatibilizer and of the filler, for this reason the final color is brown but lighter than the one of PLA-F.

From the dimensions of the diameters, it is possible to conclude that the extruded filaments were suitable to be utilized in the 3D printer, since their diameters are similar and close to the value of 1.75 mm that is the standard for the 3D printing filaments.

The PLA and PLA-C had been printed and some mechanical analysis were performed on the specimens: the tensile test with a universal machine for mechanical test and the Dynamic Mechanical Analysis (DMA). The first one is related to comprehend the resistance to stresses of the materials, as the young modulus, the maximum stress to which the material can resist, the stress applied at the breaking point and the maximum elongation at the breaking point. The DMA instead is related to the analysis of the viscous behaviour of the material, its conservative modulus (E'), its damping factor (that represents the value in which the viscous behaviour is maximum) as a function of the temperature. With these analyses it was possible to create a first

general overview about the interaction between the compatibilizer and the PLA. For this reason separated considerations about the thermal behaviour and the molecular structure of PLA and PLA-C have been performed.

3.2.1. Characterization of the filaments of PLA and PLA-C

The filaments were subjected to spectroscopic analysis ATR FT-IR to check if the blending process altered the chemistry of the two components. After the molecular characterizations, thermal analyses (TGA and DSC) were performed. The TGA analysis was performed in order to check the degradation temperatures of the components in the filament and the relative mass losses, since it is important that during the extrusion the material does not degrade, since that will cause the mechanical properties to decrease. The DSC was instead performed to check the molecular phase changes that occurred at different temperatures. It was checked the glass transition temperature, the melting point and the crystallization temperature with the related enthalpies and the degree of crystallization. The obtained values of the enthalpies of crystallization and of melting are normalized to the percentage of PLA present inside the material. In this way it is possible to understand if a component can influence the typical characteristics of PLA.

Last, a study on the hygroscopicity of the PLA and PLA-C was conducted, drying them and comparing the results of their characterization analysis in order to see if some differences are presents, if the moisture was absorbed, and to quantify it.

3.2.2. Comparison between PLA and PLA-C

The first analysis conducted is related to the spectroscopic characterization, with an ATR FT-IR, which spectra is represented in *figure 23*.

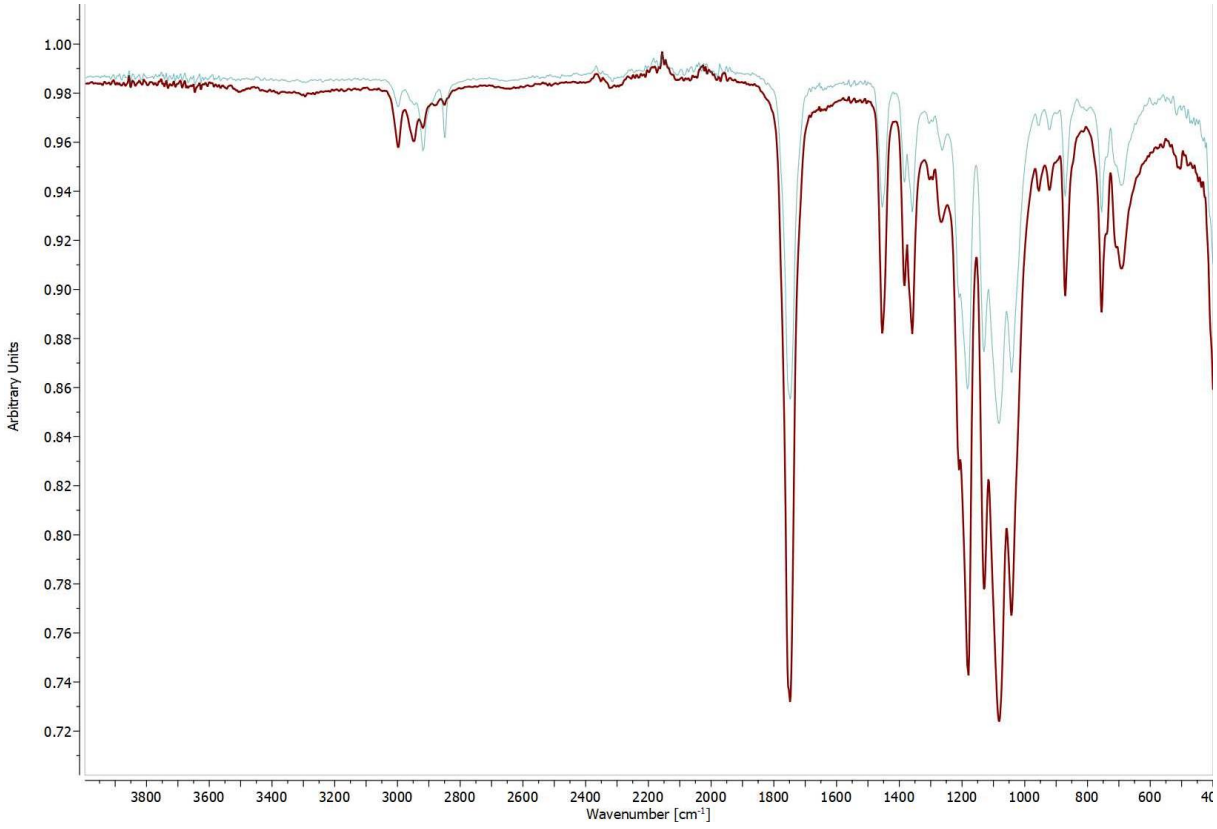

Figure 23 Comparison between PLA (red line) and PLA-C (light-blue line) FT-IR spectra

There are no substantial differences between the two spectra, since there are not shifts of the characteristic peaks, the stretch of the C=O of the ester group at 1740 cm^{-1} of the ester group and the peaks between 2850-3020 cm^{-1} that are related to the terminal carboxylic groups and to the stretch of CO-OH. The absence of significant PVA-g-LA peaks is related to the small amount of compatibilizer present inside the matrix, that does not provide very prominent absorbances.

A TGA analysis (represented in *figure 24*) was performed in order to check the degradation temperatures of the components inside the materials and the final residue.

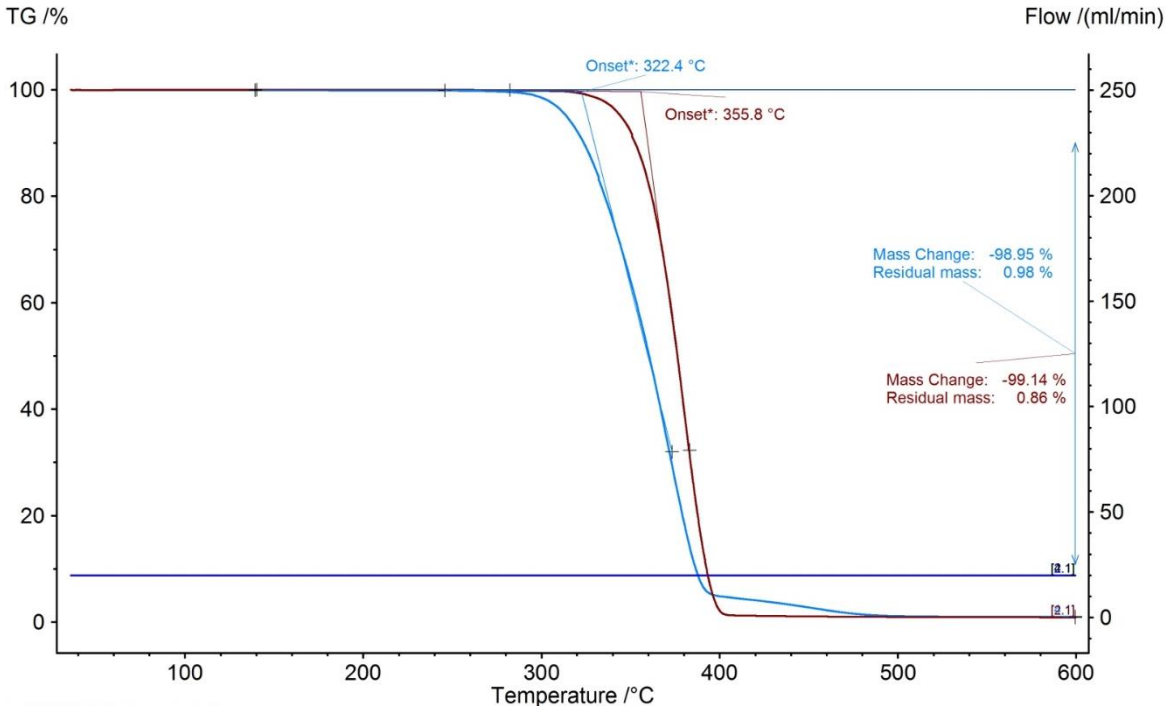

Figure 24 Comparison between the TGA thermogram of the filaments of PLA (red line) and of PLA-C (blue line)

From the TGA thermogram is it possible to obtain the data resumed in the *table 2.*

Table 2 Data obtained from the TGA thermogram of the filaments of PLA and of PLA-C

Material	**T_{onset} (°C)**	**Residue % (w/w_{tot})**
PLA	**355**	**0.8**
PLA-C	**322**	**0.9**

There is a decrease in the Temperature of degradation of the PLA-C of 33°C, that is related to the presence of the compatibilizer in the blends that has a lower degradation temperature (309°C). It is responsible also for the small increase in the residue at the end on the analysis, according to its previously described degradation pattern.

Last a DSC analysis was carried out in order to check the phase transitions and the arrangements that occurred inside the macromolecules. The thermograms are reported in *figure 25*.

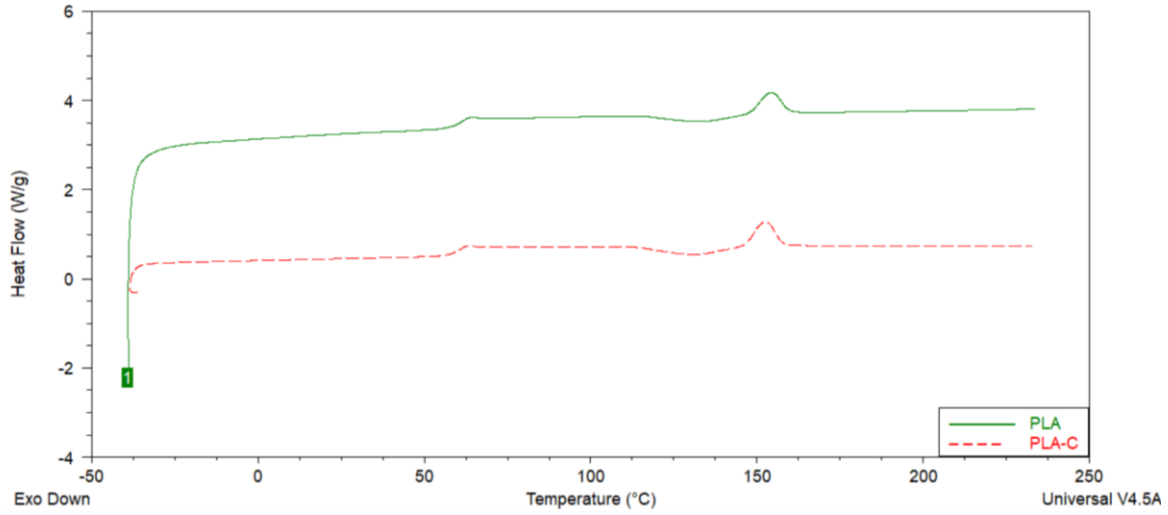

Figure 25 Comparison between the DSC thermogram of the filaments of PLA and PLA-C.

From the DSC thermogram it was possible to obtain the values resumed in the *table 1*.

Table 3 Data obtained from the DSC analysis of the filaments of PLA and PLA-C

Material	**T_g (°C)**	**T_{cr} (°C)**	**$\Delta H_{cr\ eff}$ (J/g)**	**T_m (°C)**	**$\Delta H_{m\ eff}$ (J/g)**	***X (%)***
PLA	60	115	8.6	154	10.6	2.1
PLA-C	60	113	9.1	152	10.8	1.9

It is possible to see that the glass transition temperature is unchanged, and also the crystallization and melting temperatures are practically unmodified (only 2°C difference upon the addition of the compatibilizer). Also the values of the enthalpies are comparable. The enthalpies of the crystallization and of the melting are similar, for this reason almost all the transition is related to the cold crystallization, typical of the PLA. It is related to a fraction of the macromolecule that, at the increasing temperature after the glass transition, gains mobility and are able to rearrange in an ordered fraction that will develop above the already existing crystals [45]. The degree of crystallinity (X) is overall very low, this is related to the chemical behaviour of the PLA, since it has a very low rate of crystallization, as it was said in the *chapter 1.1.1*. The lack of differences in the main PLA behaviour of the PLA-C suggest a poor interaction of the compatibilizer with the main polymeric matrix, leading to some phase separation. The fact, however, that the compatibilizer should interact with the biofillers as well, should be taken into account.

3.2.3. Estimation of the hygroscopicity of the filaments

The single materials utilized in the production of the filaments are highly hygroscopic (as it is described in *chapters 1.1.1.*, *1.2.1.* and *1.2.2.*), this influences their final properties. The water present inside the material can have many effects: it can create voids during the extrusion caused my moisture evaporation, can bond terminal groups that cannot react with the other moieties in order to improve the final properties.

Before the extrusion for the production of the filament, the single components were dried, but if in the form of wire they continue to absorb water, this could create issues during the printing, also the mechanical and thermal properties could be altered. This situation must be avoided, for this reason, some thermal analysis were performed on the filaments, to understand if it was necessary to dry the filaments and the printed samples before the tests and the quantity of water that they absorbed.

The quantity of water present in the final filament was checked performing a Thermogravimetric Analysis (TGA) and a Differential Scanning Calorimetry (DSC) on two samples, one composed by PLA and one composed by PLA-C (90:10). Each of them was put in an furnace at 120°C for 3 hours and then in a dryer for 2 hours. The temperature was chosen in order to have a temperature higher than the boiling point of water, for a time quite long in order to be sure that all the moisture had the time to evaporate. It was checked the difference between the dried filaments and the ones that were kept in environmental conditions.

The first analysis conducted is a TGA analysis. The following thermogram in *figure 26* represents the PLA filament dried and the one remained in environmental conditions.

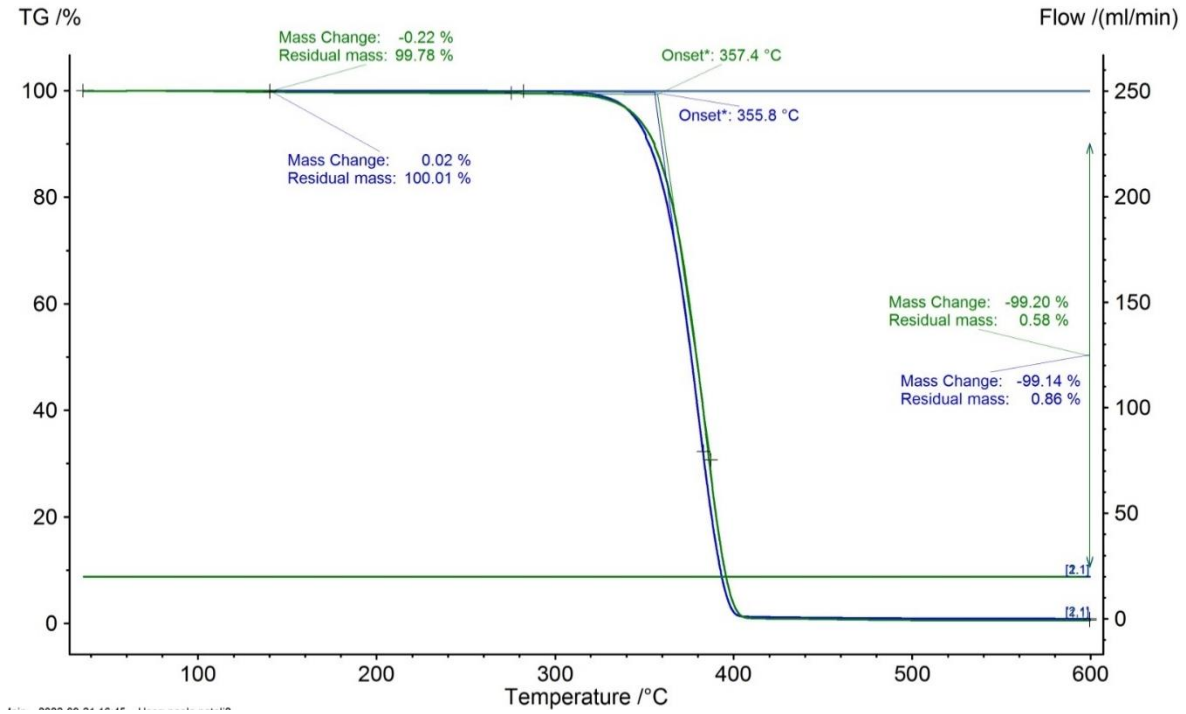

Figure 26 TGA thermogram of a filament of PLA in environmental conditions (green one) and of a filament of PLA dried (blue one)

As it is possible to see from the thermogram there is no presence of water in the PLA filament, since the loss of mass is comparable in both cases and it occurs around 350°C, is not relevant the mass lost before 150°C.

The following thermogram in *figure 27* represents the TGA analysis of the PLA-C filament, dried and in environmental conditions.

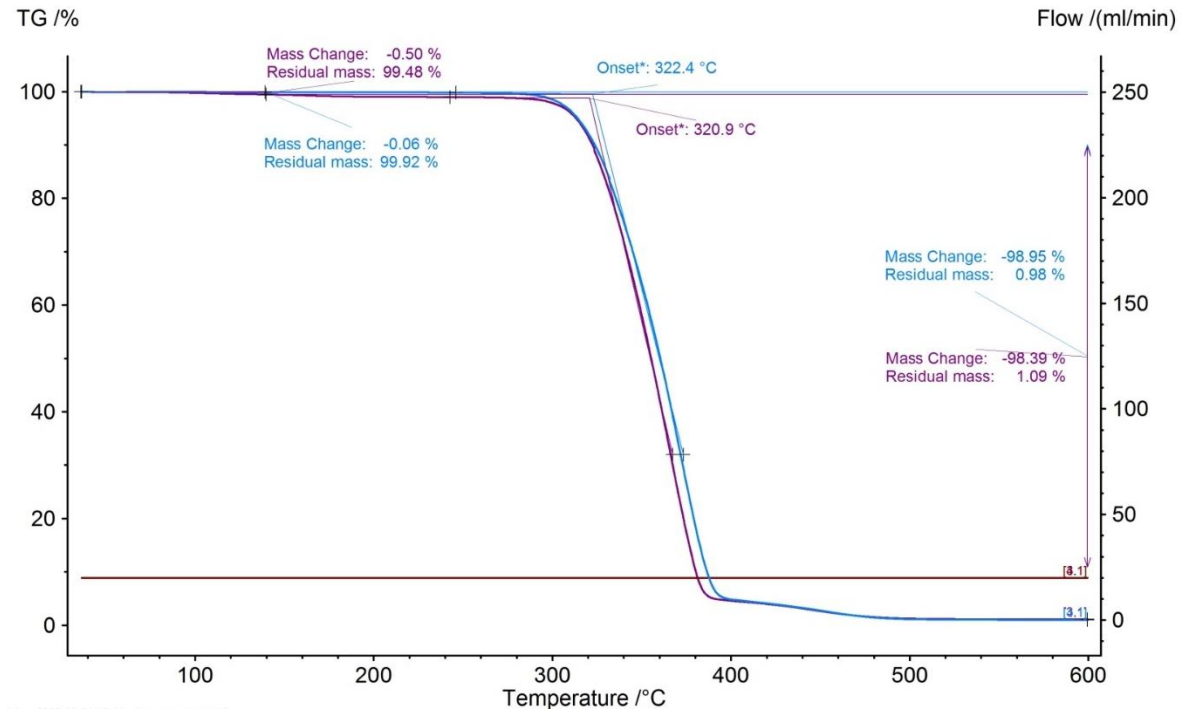

Figure 27 TGA thermogram of a filament of PLA-C in environmental conditions (violet line) and of a filament of PLA-C dried (blue line)

In the case of PLA-C the presence of water is not relevant, because the mass loss occurs in both cases around 320°C. There is no relevant change in the mass before the 150°C.

Another thermal analysis was performed as confirm, the DSC. In *figure 28* is represented the DSC on the dried PLA and on the one remained in environmental conditions. During the elaboration of the results it was considered the first heating to check the eventual quantity of water present.

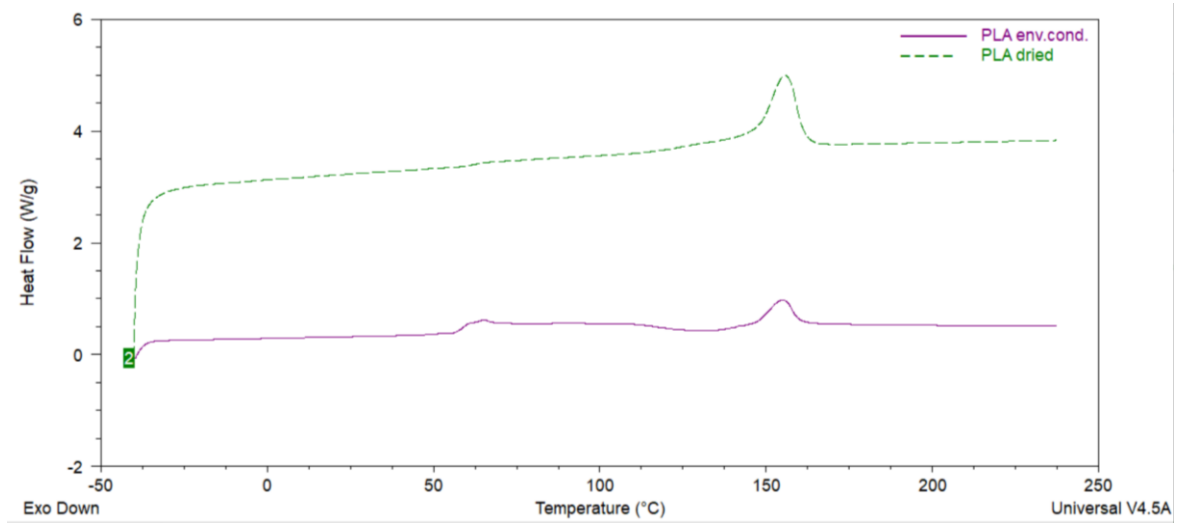

Figure 28 DSC thermogram of PLA in environmental conditions (PLA env.cond.) and the dried PLA

In the PLA thermogram it is possible to confirm that there is no presence of water, since, apart the glass transition, there are no endothermic transitions above 100 °C.

The following thermogram in *figure 29* is the DSC analysis of the PLA-C, dried and remained in environmental conditions. It was considered the first heating during the elaboration of the results.

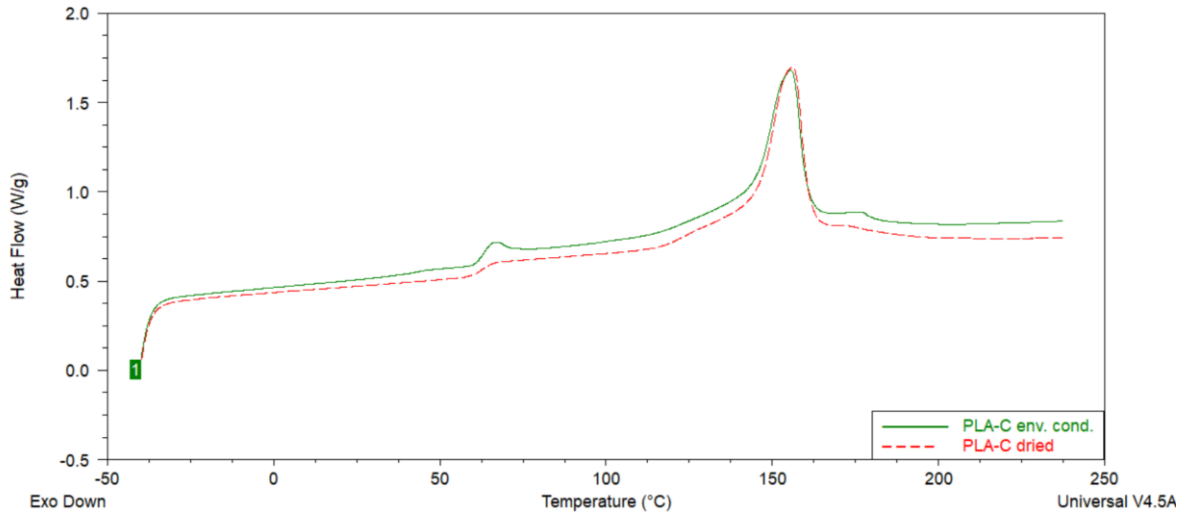

Figure 29 DSC thermogram of PLA-C in environmental conditions (PLA-C env. cond.) and the dried PLA-C

In the PLA-C thermogram there are no endothermic transitions before 100°C, apart the glass transition. It is possible to conclude that it is not detected the presence of water.

The DSC analysis for both the PLA and the PLA-C excluded the presence of water inside the filaments, and establish that a drying process before the extrusion is not necessary.

It is possible to conclude that from the thermal analysis it is not highlighted the need to dry the filaments before the printing, in both the cases of PLA and of PLA-C. This will reduce the energy required to produce the final object, and so the costs and the environmental impact. Also, the time will be lower, so the efficiency of the production process will increase.

3.3. 3D printing

In order to further increase the sustainability of the production of the new material, the filaments was processed with the FDM technology. Compared to the injection molding, this method produces a lower number of wastes, is easier and reduce the time required to the creation of the final object, as it was previously reported in the *chapter 1.3*.

All the samples were printed along the X axis (on the edge) with a deposition angle of 0° and of 90° as represented in *figure 30.*

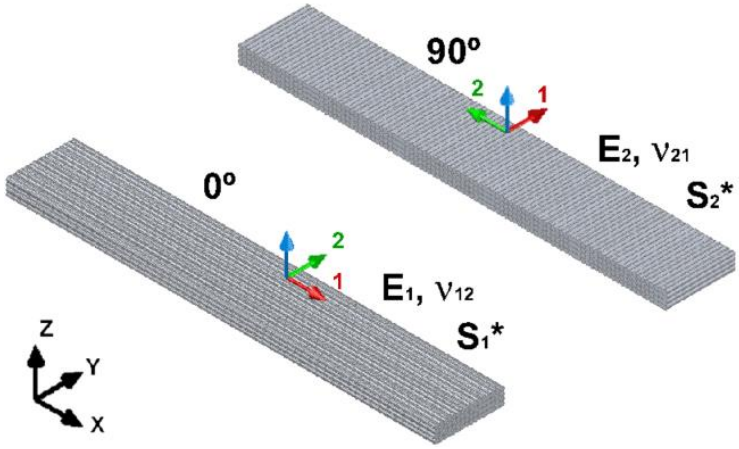

Figure 30 Representation of the angle of deposition during the printing of the samples.

It was decided to maintain the X axis direction of printing since is the one that always shows higher performances of the printed specimens (as it was previously reported in the *chapter 1.3.1*), and it was considered of major relevance the angle of deposition.

It is expected that the samples printed along the 0° direction will have higher mechanical properties, since the layer are oriented along the direction of the stress. Instead, the ones printed along the 90° direction will be subjected to the stress forcing the junction of the layers, that are more fragile since the interactions between the macromolecules are weaker, since they are aligned along the printing direction, as it was previously described in the *chapter 1.3.1*

It is also expected that the samples that do not contain the compatibilizer will have higher mechanical properties, since the role of the compatibilizer is not to increase the tensile resistance of the material (as it was previously reported in the *chapter 1.2.1.*), but to be an intermediate between the matrix (PLA) and the filler, decreasing the energy of the interlayer and stabilizing it, decreasing the anisotropy of the material and increasing its mechanical properties.

3.3.1. Printing of the samples

An optimization of the printing parameters of the samples of PLA and PLA-C was performed, in order to improve their mechanical properties.

The preparation of the 3D printer was performed with the following procedure: the filament of the material was inserted into the chamber of extrusion and the wire feeder was set depending on the hardness or softness on the material (in the case of PLA, the value was the one related to the harder materials). The bed must be clean and a layer of lacquer was applied in order to prevent the specimen to stick to the bed. The lacquer must be applied to at least 20 cm distance from the bed in order to avoid the formation of drops on it.

The instrument was ready to read the first file elaborated from the slicer that contained all the printing information and to produce the first object.

The object was first created with a CAD software (FreeCAD), in which the shape and the dimensions were defined, and it was saved as .std format file. Then with another software, the slicer (Simplify3D), all the printing parameters were defined, and it was converted in a .stl format file that could be read by the 3D printer.

The 3D printer read the file and elaborated all the contained information and started to create the object.

During the optimization of the printing parameters the temperatures were set directly on the 3D printer during the production of some samples. The speed instead must be set on the slicer.

The optimization for the PLA-C printing presented some issues, since it was more difficult to produce some samples without voids or some empty layers. This was related to the discontinuous diameter of the filament, and to the fact that the presence of two substances inside the filament (and so the contribution of the compatibilizer) created, even if in small part, anisotropy along the material, and so the temperatures and the properties were not completely constant along all the filament.

3.3.2. Characterization of the printed samples

The samples of PLA and of PLA-C printed with an angle of deposition of 0° and of 90° were characterized with a tensile test by the utilisation of a dynamometer. The results are represented in *figure 31*.

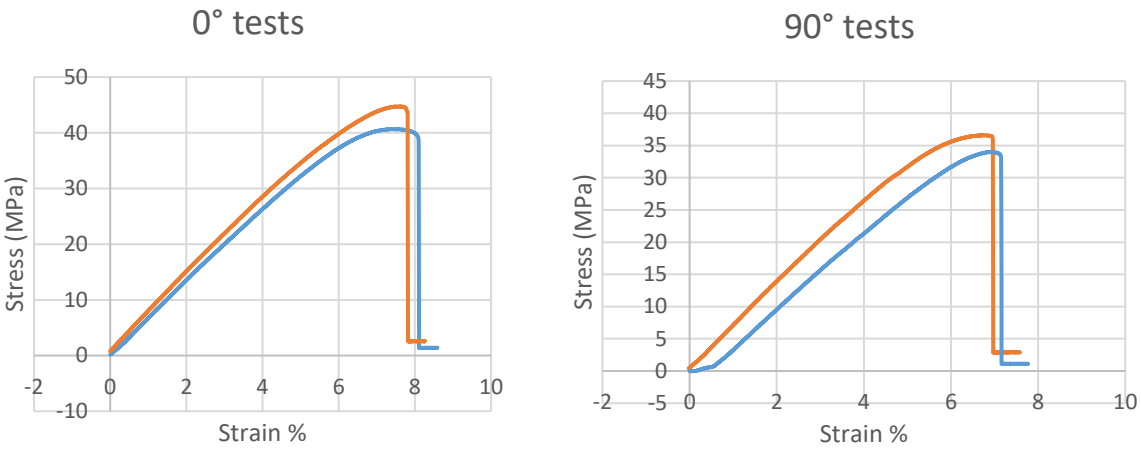

Figure 31 Results of the tensile tests (respectively at 0° and 90° printed samples) of PLA (orange line) and PLA-C (blue line)

The values obtained are represented in the graphs in *figure 32* and resumed in the *table 4.*

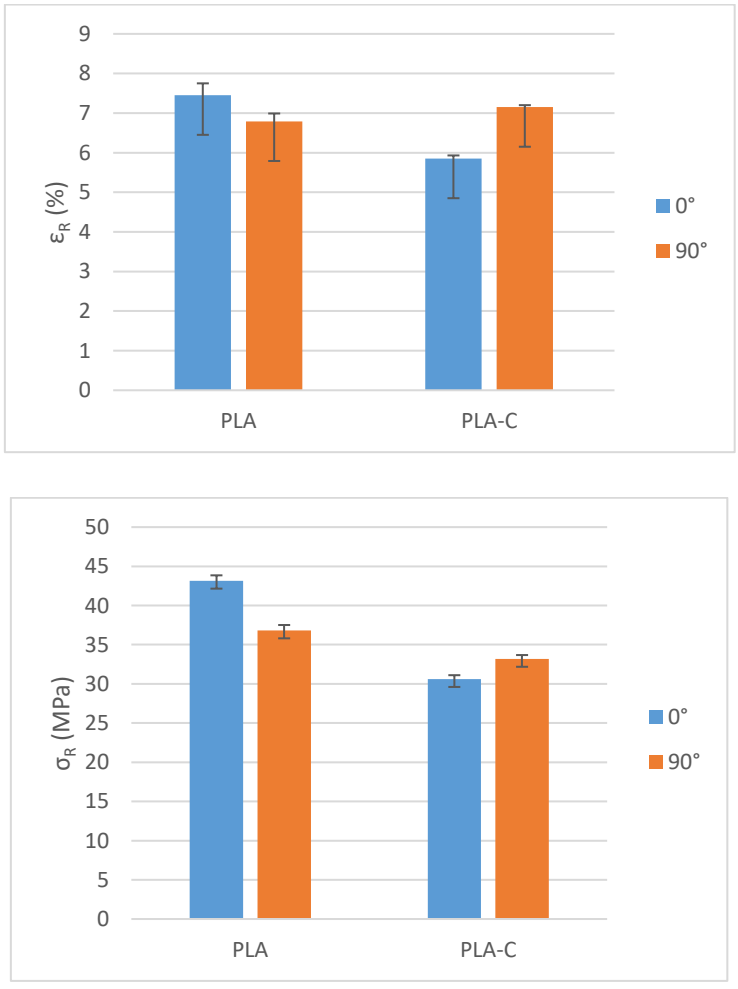

Figure 32 Charts representing the elongation at break (ε_R) and the stress at breaking (σ_R) values for the specimens of PLA and PLA-C printed at 0° and at 90°

Table 4 Mean values obtained from the tensile test for the printed samples of PLA and PLA-C, printed ad 0° and at 90°

	E' (MPa)	**σ_{max} (MPa)**	**σ_R (MPa)**	**ε_R (%)**
PLA 0°	771 ± 6	44 ± 1	43 ± 1	7.4 ± 0.3
PLA 90°	675 ± 2	37 ± 1	37 ± 1	6.8 ± 0.2
PLA-C 0°	604 ± 4	31 ± 1	31 ± 0.5	5.8 ± 0.1
PLA-C 90°	479 ± 8	34 ± 2	33 ± 0.5	7.2 ± 0.1

The PLA printed with a deposition angle of 0° presented an elastic modulus E' of 771 MPa, the value of the maximum stress applied was 44 MPa and the stress applied at the breaking point was 43 MPa. The elongation at break was 7.4%.

The PLA printed with a deposition angle of 90° showed a drop in the elastic modulus E' of 675 MPa, lower than the one of PLA printed at 0° as it was expected. The maximum stress applied was 37 MPa, once again lower than the one of PLA printed at 0°, as the stress applied at the breaking point, that has a value of 37 MPa. Also, the elongation at break is lower than the one of the PLA printed at 0°, with a value of 6.8%. For the PLA, it is confirmed that the sample printed with a deposition angle of 90° presented a general decrease in the mechanical properties.

The PLA-C printed with a deposition angle of 0° presented an elastic modulus E' of 604 MPa, the maximum stress applied was of 31 MPa and the stress applied at the breaking point was of 31 MPa. All the values obtained are lower than the ones of the PLA printed at 0°, as it was expected, since the compatibilizer acts as an impurity in the material and cause a decrease in the mechanical properties. Also, the elongation at break was lower than the one of PLA printed at 90°, since it had a value of 5.8%.

The PLA-C printed with a deposition angle of 90° showed an elastic modulus of 479 MPa, lower than all the other printed materials, for the additional effect of the presence of the compatibilizer, that acted as impurity, and to the printing direction, since the stress was applied perpendicularly to the printing direction and involved the interlayers, that are the weakness in the FDM technology, as it was previously reported in the *chapter 1.3.1*. The maximum stress applied, with a value of 34 MPa, and the stress applied at the breaking point, with a value of 34

MPa, were instead higher than the one of the PLA-C printed at 0°, but still lower than the ones of the PLA printed at 90°. The elongation at break was instead higher than both the PLA printed at 90° and the PLA-C printed at 0°, but lower than the PLA printed at 0°, with a value of 7.2%.

It was confirmed that the compatibilizer does not increase the strength of the material, but when the filler is not present it acts as an impurity in the matrix, and overall, the PLA is damaged by its presence. Also, the direction of printing has a large influence on the mechanical properties, since they were generally decreased with a deposition angle of 90°.

Another mechanical test was carried out, the dynamic mechanical analysis (DMA). It was performed to extrapolate the values of the conservative module (E'), of the temperature of onset at which there is the decrease of E' and the temperature of the peak of *tanδ* that represents the temperature at which damping factor is maximum. The analysis was performed on the samples printed with a deposition angle of 0° and of 90° of PLA and of PLA-C.

The following graph in *figure 33* is related to the DMA analysis of the PLA and of the PLA-C printed with a deposition angle of 0°.

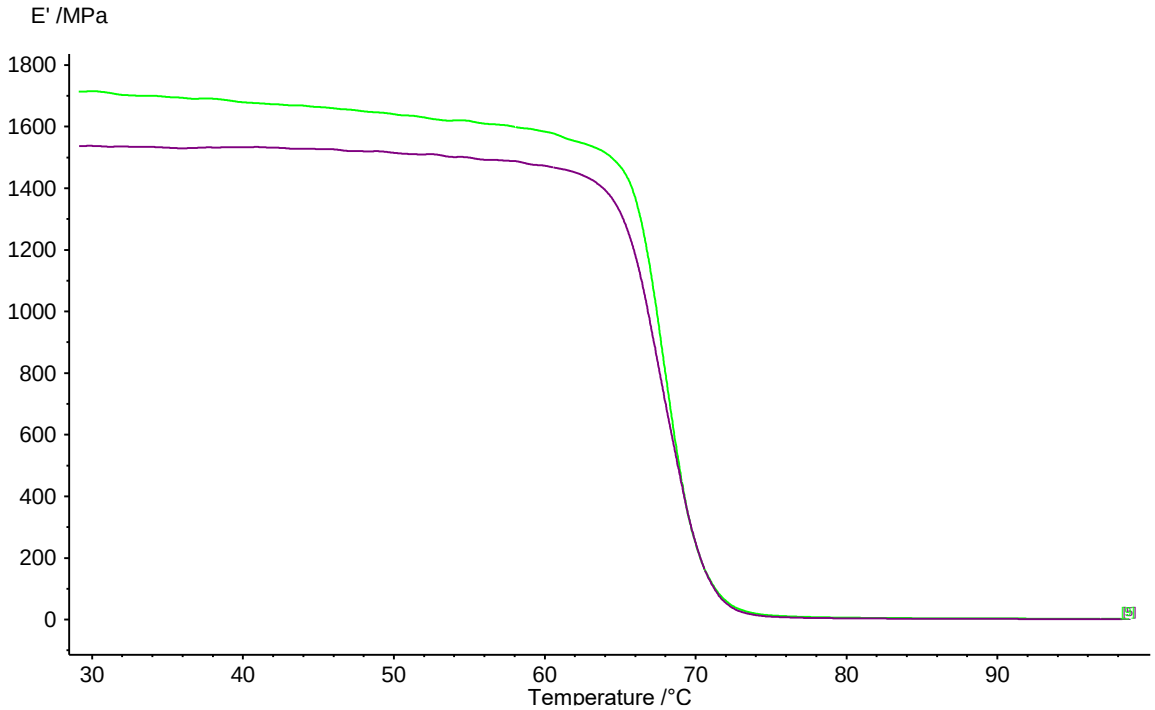

Figure 33 Results of the DMA test of PLA (violet line) and PLA-C (green line) printed at 0°

The values obtained from the graphs are in resumed in the *table 5*.

Table 5 Mean values obtained from the DMA measurements of the printed samples of PLA and PLA-C at 0°.

Material	Module E' at 30°C (GPa)	T_{onset} (°C)	Peak of tanδ (°C)
PLA	1.6 ± 0.2	65 ± 2	75 ± 3
PLA-C	1.9 ± 0.2	65 ± 1	74 ± 1

The PLA showed a conservative module E' of 1.6 GPa, a temperature of start of drop of E' of 65 °C and a value of peak of tanδ of 75 °C.

The PLA-C presented a conservative module E' of 1.9 GPa, a temperature of start of drop of E' of 65 °C and a value of peak of tanδ of 74 °C. The module is higher than the one of the PLA, possibly owing to the type of external stimulus that is applied. Indeed in DMA the sinusoidal force application within the elastic deformation of the component is not negatively impacted by voids, as much as it is in the stress/strain tests, where voids actively trigger cracks and failures thus leading to anticipated drops of performance. These two opposite results might thus suggest that the presence of the compatibilizer could not be that detrimental of the final blend mechanical performance, once the voids issue deriving from the processing will be solved.

The next DMA analysis is focused on the PLA and PLA-C specimens printed with a deposition angle of 90°. The results are represented in *figure 34*.

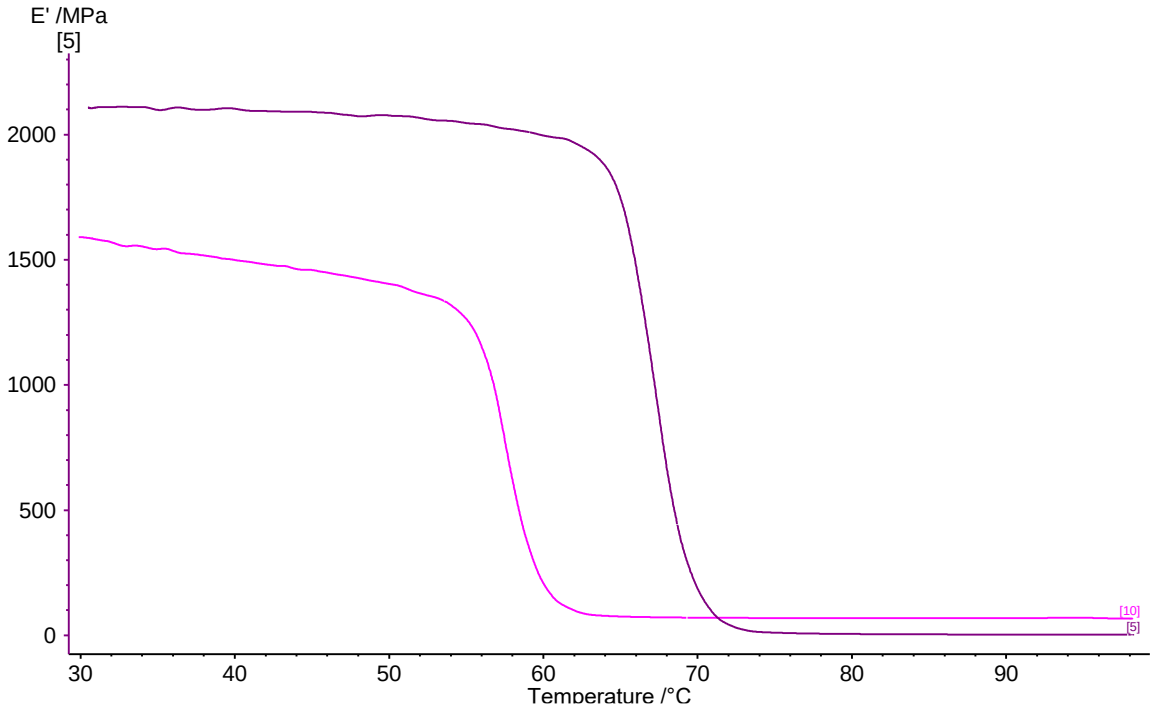

Figure 34 Results of the DMA test of PLA (violet line) and PLA-C (pink line) printed at 90°

The values obtained from the graphs are in resumed in the *table 6*.

Table 6 Mean values obtained from the DMA measurements of the printed samples of PLA and PLA-C at 90°.

Material	**Module E' at 30°C (GPa)**	**T_{onset} (°C)**	**Peak of tanδ (°C)**
PLA	1.6 ± 0.1	65 ± 1	74 ± 1
PLA-C	1.5 ± 0.1	66 ± 1	66 ± 1

The PLA showed a conservative module E' of 1.6 GPa, a temperature of start of drop of E' of 65 °C and a value of peak of tanδ of 70 °C. The values are very similar to the ones of the PLA printed with a deposition angle of 0°, so it is possible to conclude that, for the PLA, the deposition angle did not influence its viscous properties.

The PLA-C showed a conservative module E' of 1.5 GPa, a temperature of start of drop of E' of 66 °C and a value of peak of tanδ of 66 °C. The module and the peak of tanδ are lower than the one of the PLA, this can be related to the presence of the compatibilizer that acted as impurity and decreased the properties of the matrix, since its function is not to reinforce the material, but to decrease the energy of the interphase between the filler and the matrix in a biocomposite (as it was previously reported in the *chapter 1.2.1*). The obtained values are lower than the one of the PLA-C printed with a deposition angle of 0°, this can be related to the optimization of the printing parameters, that was perfectly performed along that direction but not when the deposition angle is of 90°.

3.4 Extrusion of the PLA-C-F filaments

The PLA-C extrusion was correctly performed, producing a filament suitable for the 3D printing. It was proceeded with the extrusion of the PLA-C-F filament, for which the results were not so positive.

When a third component was added to the extrusion, so with the addition of the filler, it was impossible to spool the filament. It presented a very brittle behaviour and a very low diameter, as it is possible to see in *figure 35*. A second extrusion did not improve this behaviour. An

attempt at varying the concentration of the compatibilizer, ranging from 2%, 5% and 10%, lead to no substantial physical differences in the product of the extrusion.

Figure 35 product of the extrusion of PLA-C-F 85:5:10

The reason is related to the fact that the bonding between the compatibilizer and the cellulose probably did not occur. As it was previously said in the *chapter 1.2.2.,* cellulose is a quite inert material, since its -OH groups are not exposed to the surface, and it's very difficult that they interact with other molecules, due to their hydrogen bonds between alcoholic groups.

Characterization analysis were executed to all the filaments, in order to check their main differences and the relative influences of their components. It was chosen to utilize the PLA-C10-F10 among the other composition of matrix-composite-filler, since being the one with the higher quantity of PVA-g-LA it should present the major differences in the characterizations.

Then, each of the PLA-C-F filaments has been characterized to check if there were some chemical differences between the interaction of the components with a lower quantity of compatibilizer, and to try to understand the chemistry that did not allow a performant extrusion of them.

3.4.1 Comparison between the filaments

A comparison between all the filaments was performed, in order to check the main differences that can be due to the components present inside the various materials. First a spectroscopic analysis was performed with a ATR FT-IR (represented in *figure 36*).

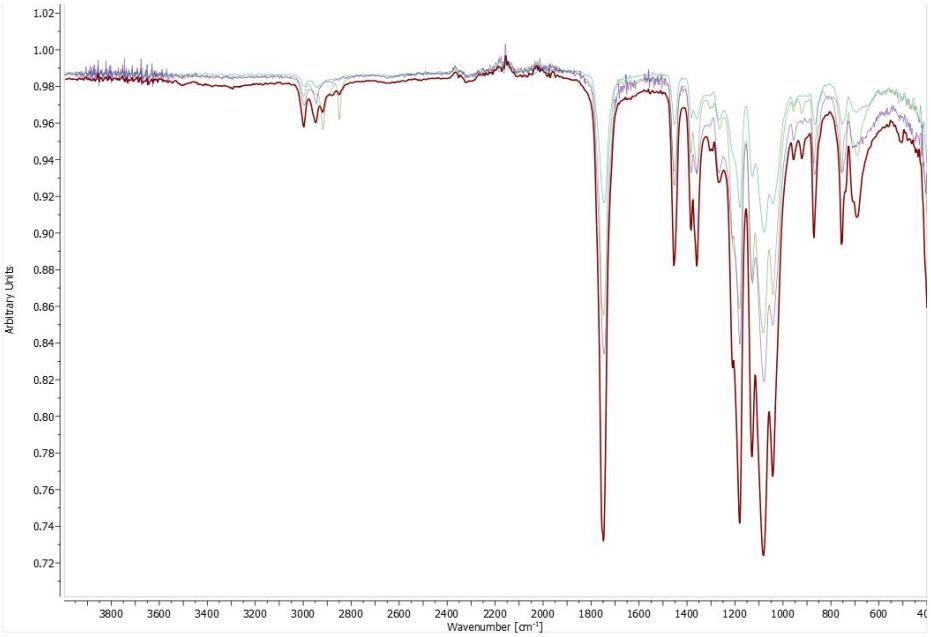

Figure 36 Comparison between PLA (light-blue one), PLA-C (red one) and PLA-F10 (violet one) and PLA-C10-F10 (green one) FT-IR spectra

No significant differences between the spectra of the different materials were detected. The characteristic peak of the ester bond at 1860 cm^{-1} related to the stretch of the C=O is in the same position for all the filaments, as the peaks in the region between 2840-3020 cm^{-1} related to the stretch of the CO-OH of the terminal carboxylic groups. The absence of differences can be related to the small amount of filler and compatibilizer with respect to the matrix, that are not visible with this instrument.

A TGA analysis (in *figure 37*) was performed, in which the degradation temperatures and the residual mass of the different materials were compared, in order to evaluate the relative influence that the single components cause to the properties of the PLA.

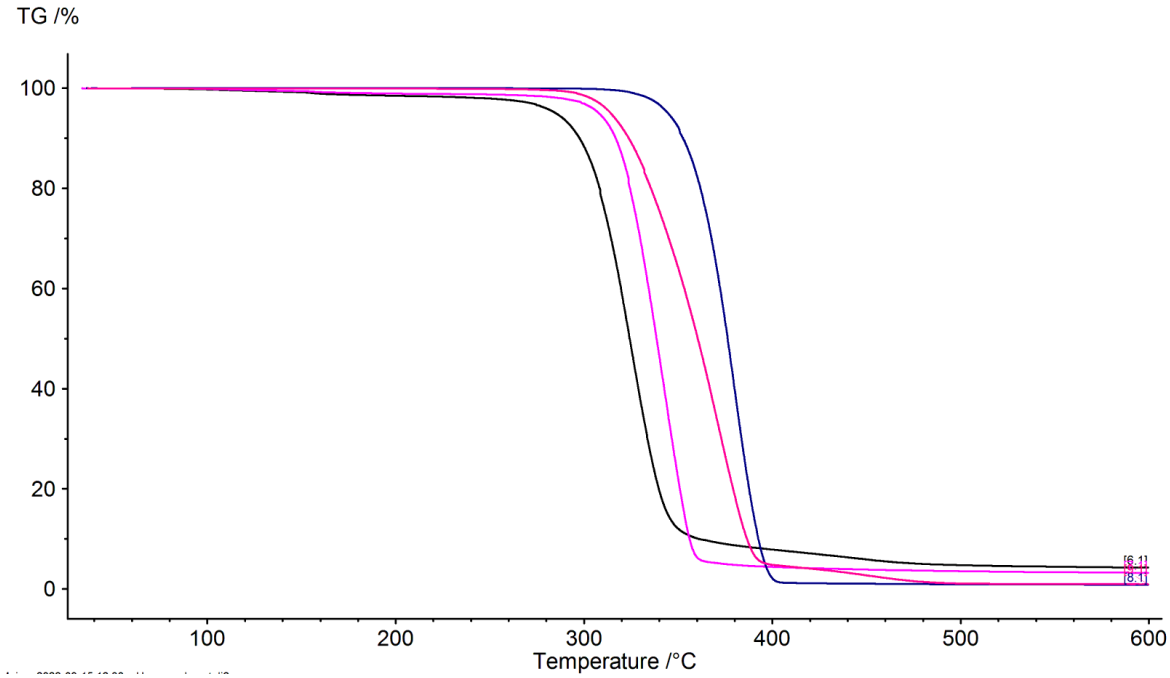

Figure 37 comparison between the TGA thermogram of PLA-C10-F10 (black line), PLA (blue line), PLA-C (red line) and PLA-F (rose line)

It was possible to obtain the data contained in the *table 7* from the TGA thermogram of the filaments.

Table 7 Data obtained from the TGA thermogram of the filaments

Material	T_{onset} (°C)	Residue % (w/w_{tot})
PLA	354	0.7
PLA-C	322	1.0
PLA-F	316	3.1
PLA-C10-F10	299	4.0

The PLA-F thermogram showed a temperature of start of degradation at 316.3°C, lower than the one of the PLA and of the PLA-C, related to the degradation temperature of the filler that is lower than the one of the PLA (as it was said the *chapter 1.2.2.*, the cellulose degrade above 200°C). The residue was 3.1%, higher than the one of PLA and PLA-C since the filler remained as degraded fraction in larger amount after the thermal treatment at 60°C.

The PLA-C-F analysis showed a temperature of initial degradation of 299°C, lower than all the other filaments, related to the additional effect of the filler and of the compatibilizer. The residue was 4%, higher than all the others for the remained degraded fraction related to the filler (present in larger amount) and of the compatibilizer.

DSC (in *figure 38*) were then carried out in order to compare the temperatures of the glass transition, of the melting and of the crystallization of all the materials and the related enthalpies. Also the degree of crystallinity is considered. It is evaluated if the presence of other components influences the characteristic properties of the matrix (the PLA).

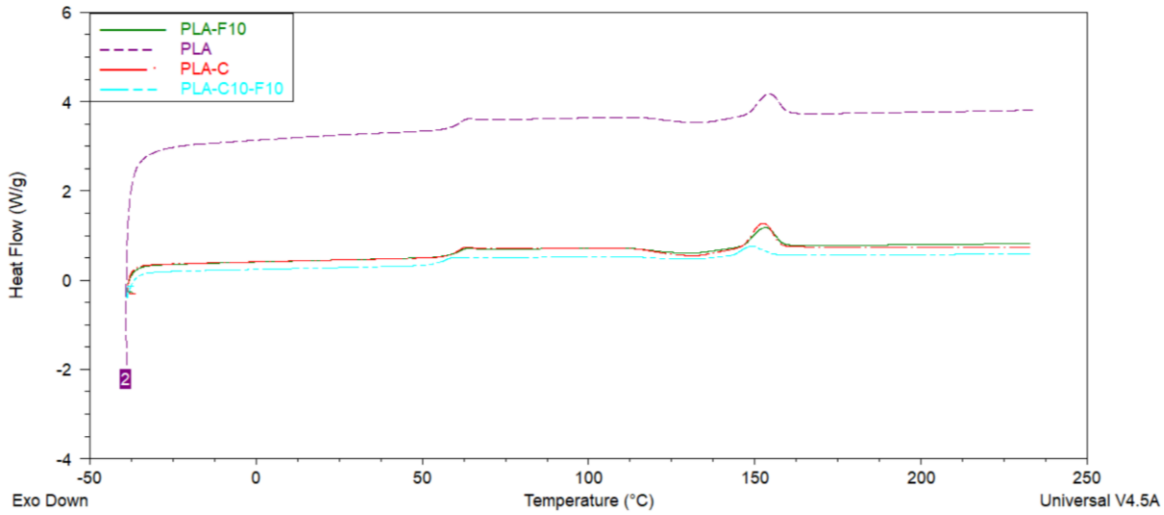

Figure 38 Comparison between the DSC thermogram of PLA, PLA-C, PLA-F and PLA-C10-F10

The data obtained from the thermogram are resumed in the *table 8*.

Table 8 Data obtained from the DSC analysis of the filaments

Material	**T_g (°C)**	**T_{cr} (°C)**	**$\Delta H_{cr\ eff}$ (J/g)**	**T_m (°C)**	**$\Delta H_{m\ eff}$ (J/g)**	***X (%)***
PLA	60	115	8.6	154	10.6	2.1
PLA-C	60	113	9.1	152	10.8	1.9
PLA-F	60	112	7.6	153	8.6	1.1
PLA-C10-F10	55	113	3.1	149	4.3	1.3

The PLA presents a glass transition temperature at around 60°C, its crystallization temperature is 115°C and the melting temperature is 154°C. The enthalpies of crystallization and of melting are similar (8.6 J/g and 10.6 J/g), so the transition is largely related to cold crystallization. The degree of crystallinity is 2.1%, quite low, but this is related to the properties of the PLA and to its extremely low speed of crystallization. This observation, however, is a premium quality in the filament for 3D printing, where an excess of crystallinity might impart an extreme stiffness to the filament causing issues in drawing it from the spool during the additive manufacturing process.

The previous discussion in the *chapter 3.2.2*. evidenced that the compatibilizer addition did not affect PLA behaviour, suggesting a phase separation of the two components in the bled; the attempt at adding only the biofiller also had small impact on PLA behaviour.

Indeed, PLA-F thermal analysis shows a glass transition temperature at around 60°C (as the one of the PLA, a crystallization temperature of 112°C and a melting temperature of 153°C. They are slightly lower than the temperature of the PLA, as well as the enthalpies of crystallization and of melting are similar (7.6 J/g and 8.6 J/g, respectively). This can be related to an effect of the filler, that further decreased the ability of the PLA to crystallize, requiring more time.

The PLA-C-F filament was the last analysed with the DSC and showed a glass transition temperature at around 55°C, lower than the one of the PLA and of the other filaments. This effect might be related to the interaction matrix-compatibilizer-filler. The crystallization temperature was 113°C, while the melting temperature was 149°C, lower than the one of the PLA for the nucleating effect of both the compatibilizer and the filler. The enthalpies of crystallization and of melting were respectively 3.1 J/g and 4.3 J/g, mainly related to the cold crystallization effect. They were lower than the one of the PLA, possibly due to some detrimental effect of the compatibilizer on the PLA matrix and on the presence of the biofiller that is hampering the crystallization.. The degree of crystallinity was 1.3%, lower than the one of the PLA, since there is a lower amount of material inside the composite that is able to crystallize (only the 89%), and due to the effect of the filler.

3.4.2. Comparison between the PLA-C-F filaments

The filaments of PLA-C-F with different concentrations of compatibilizer were then characterized, with thermal analysis and with a spectroscopic analysis with a ATR FT-IR, in *figure 39* it is reported the obtained spectra.

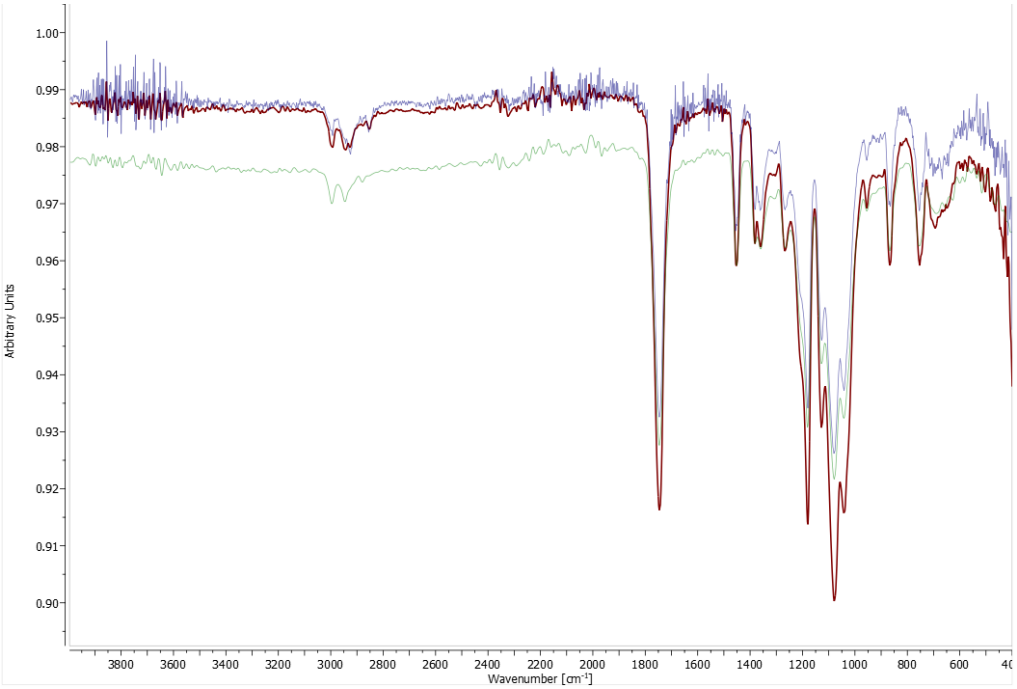

Figure 39 Comparison between PLA-C10-F10 (green one), PLA-C5-F10 (blue one) and PLA-C2-F10 (red one) FT-IR spectra

It is possible to see a difference in the intensity of the peaks, increasing with the quantity of the compatibilizer, mostly of the carboxylic peak at 1750 cm^{-1}. The characteristic peaks are the same for all the samples, the stretch of the C=O of the ester group at 1740 cm^{-1} and the stretch of the CO-OH of the terminal carboxylic groups between 2850-3020 cm^{-1}. There are no other differences but the increasing of the intensity of the peaks.

A thermal characterization was performed on all the samples of PLA-C-F, a TGA analysis (represented in *figure 40*), in order to understand the influence that the variation of the quantity of compatibilizer caused to the biocomposite. It was analysed the temperature of start of degradation and the final residue after a thermal treatment at 600°C.

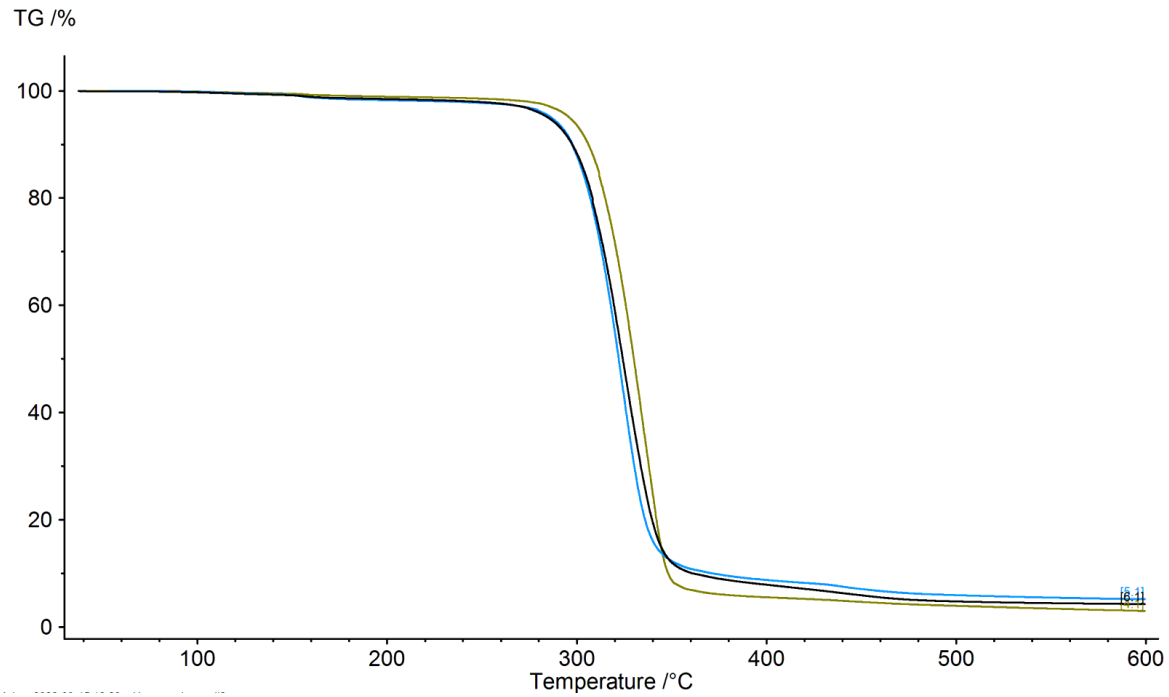

Figure 40 comparison between the TGA thermogram of PLA-C2-F10 (blue line), PLA-C5-F10 (green line) and PLA-C10-F10 (black line)

From the thermogram it is possible to obtain the data written in the *table 9*.

Table 9 Data obtained from the TGA thermogram of the filaments of PLA-C-F with different concentrations

Material	**T_{onset} (°C)**	**Residue % (w/w_{tot})**
PLA-C2-F10	300	4.5
PLA-C5-F10	309	1.7
PLA-C10-F10	299	4.0

The PLA-C2-F10 thermogram presented a temperature of start of degradation of 300°C, and a residue of 4.5%, due to the presence of a degraded fraction of the filler and to the compatibilizer.

The PLA-C5-F10 showed a temperature of start of degradation of 309°C and a residue of 1.7%.

The PLA-C10-F10 presented a temperature of start of degradation of 299°C and a residue of 4%.

The presence of both the filler and the compatibilizer inside the biocomposite influence the temperature of initial degradation and the residue of the material, but it is not possible to establish a trend depending on the relative quantity of the compatibilizer.

Another thermal characterization was performed, a DSC (reported in *figure 41*) to study the effect of the relative quantities of the compatibilizer on the biocomposite transitions and crystallinity degree.

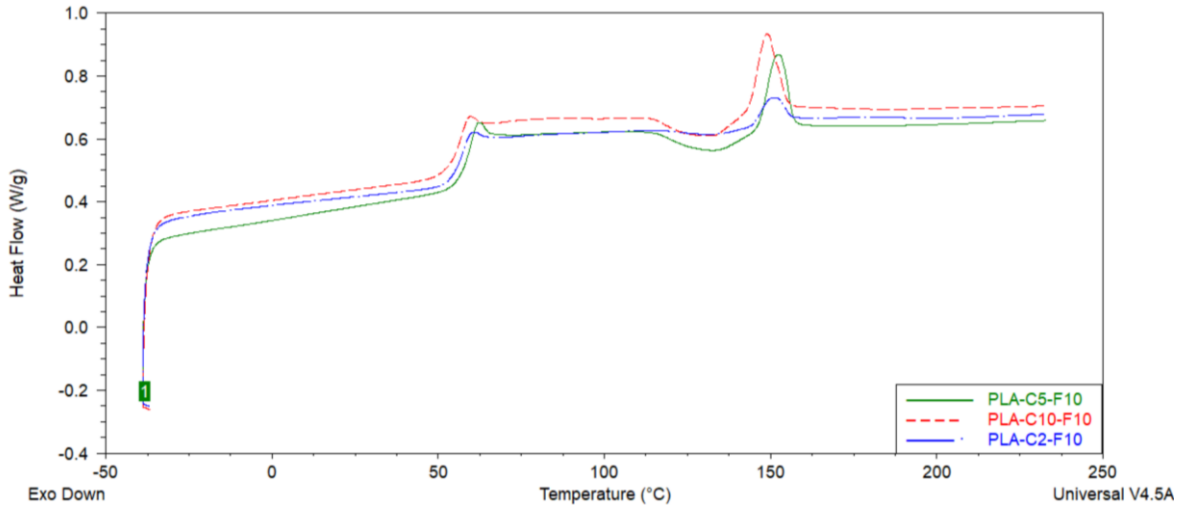

Figure 41 Comparison between the DSC thermogram of the PLA-C-F with different concentrations.

As it is possible to see, there are differences between the filaments, with an increasing of the intensity of the transitions related to the quantity of compatibilizer that they contained.

The data obtained from the graph are resumed in the *table 10*.

Table 10 Data obtained from the DSC analysis of the filaments of PLA-C-F with different concentrations

Material	**T_g (°C)**	**T_{cr} (°C)**	**$\Delta H_{cr\ eff}$ (J/g)**	**T_m (°C)**	**$\Delta H_{m\ eff}$ (J/g)**	***X (%)***
PLA-C2-F10	56	115	1.4	150	1.5	0.1
PLA-C5-F10	58	114	3.5	152	4.1	0.6
PLA-C10-F10	55	113	3.8	149	4.3	1.3

The PLA-C2-F10 presented a glass transition temperature around 56°C, a crystallization temperature of 115°C and a melting temperature of 150°C. The difference in the enthalpies of the crystallization and of melting was around 0 (the one of crystallization was 1.4 J/g and the one of melting was 1.5 J/g), so the transition was almost all related to the cold crystallization.

The degree of crystallinity was very low, 0.1%, so the crystal phase was almost completely absent.

The PLA-C5-F10 thermogram showed a glass transition temperature around 58°C, a crystallization temperature of 114°C and a melting temperature of 152°C. The enthalpy of crystallization was 3.5 J/g while the one of melting is 4.1 J/g. Their difference was almost zero, so the transition was almost all related to the cold crystallization. The degree of crystallinity was very low, only 0.6%.

The PLA-C10-F10 analysis presented a glass transition temperature around 55°C, a crystallization temperature of 113°C and a melting temperature of 149°C. The enthalpy of crystallization was 3.8 J/g and the one of melting was 4.3 J/g. The degree of crystallinity was 1.3%.

The compatibilizer caused some effects in the transitions of the biocomposite, but it is not possible to define a trend depending on its relative quantity probably owing to a lack of real compatibilization occurring during the mixing.

4. CONCLUSIONS

In this dissertation it was discusses the potential optimization of a biocomposite material with the utilization of a compatibilizer to increase their interphase adhesion, and consequently the mechanical properties of the material. Initially, the synthesis of the compatibilizer, based on PVA-g-LA was correctly carried out with an high degree of functionalization (71%).

Such a materials was used in blend with PLA to obtain different filaments, in order to make a comparison and better understand the relative influence of the single components: PLA, PLA-C, PLA-F, PLA-C-F (where C stands for compatibilizer and F for filler).

The PLA-C filament was correctly extruded. Since PLA and PLA-C absorb a large quantity of water, an hygroscopic study was performed on them. The study confirmed the absence of water, and so the drying was not necessary before the production of the specimens with the 3D printer, since water could interfere with the performance of the FDM and with the mechanical properties of the final printed samples.

The specimens were printed with different angle of deposition, at 0° and at 90°, in order to understand the relative influence of the interlayer energy with mechanical analysis. The analysis confirmed that the samples printed at 90° presented lower mechanical properties than the ones printed at 0°. The PLA-C showed a decrease in the mechanical properties with respect to the PLA, because its function is not to increase them, but to increase the interaction between the filler and the matrix when it is present.

The filament of the biocomposite PLA-C-F was extruded, but it was not possible to produce a material suitable for the FDM. As it was reported in the *chapter 1.2.2.*, cellulose is an inert material, due to the low reactivity of the -OH groups, already involved in hydrogen bonds among them. For this reason the compatibilizer was not able to interact with cellulose, and what was finally extruded was an inhomogeneous material, where the matrix and the PVA-g-LA were bonded but the filler was not. This created a large anisotropy, that lead to the extrusion of a very brittle filament with an uneven diameter. Further studies could consider this thesis as a base, maintaining the utilization of a compatibilizer and performing additionally a surface treatment on the wheat middling. The surface treatment purpose is to expose the reactive groups of the cellulose and increase its tendency to create bonds with other molecules. An alkali treatment is the most common and most simple to perform [27]. After this surface modification, the PVA-g-LA will be able to bond to the -OH groups of the cellulose and to the reactive groups

of the PLA, decreasing the interphase energy and improving the mechanical properties of the final biocomposite. This will lead to the production of a completely biobased material, resistant, with properties that will compete with the main fossil-based materials. It will be less expensive, composed by wastes that do not compete with food and so it will not create environmental or social issues.

While it was not possible to obtain a final 3D printed biocomposite, this work advocate for the need for new potential compatibilizers in order to use waste products in biobased matrices for decreasing the cost of such products. A further effort is still required to obtain better performances that will bring this approach to an acceptable level of properties to replace the presently costly sustainable polymers.

5. EXPERIMENTAL METHODS

5.1. Materials

For the synthesis of the compatibilizer they were used levulinic acid ($C_5H_8O_3$, 98%), oxalyl chloride ($C_2Cl_2O_2$, >98%), dichloromethane (CH_2Cl_2, ≥99.8%), N,N-Dimethylformamide (DMF, ≥99.8%), ethyl ether and polyvinyl alcohol (Mw: 13000-23000). All the materials were provided by Sigma-Aldrich and did not require further purifications.

As matrix was used polylactic acid IngeoTM 4043D (Nature Works, USA).

The biofiller utilised was wheat middling (diameter between 0.2 and 0.4 mm), an agri-food waste, kindly granted by the company Molino Pivetti (Italy).

5.2. Instruments

Different instruments have been utilized, for the characterization of the materials and of the filaments, for the extrusion of the filaments, for the production of the specimens, and for their mechanical test.

5.2.1. Extrusion of the filaments

The filaments were produced with the single screw extruder Advanced 4.0 (3Devo, Holland) represented in *figure 42*.

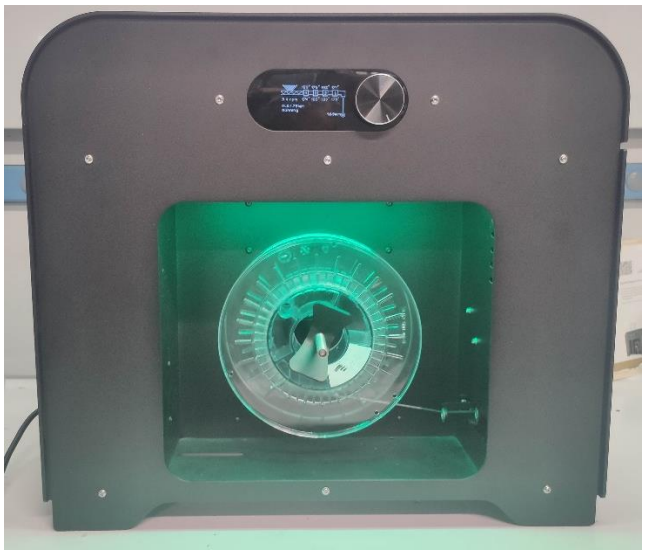

Figure 42 Extruder Advanced 4.0 during an extrusion

The extruder is composed by a loading part, in which the pellets are introduced, at its bottom there is a screw that rotate and make go ahead the pellets. Proceeding along the instrument, the material pass through four different areas, each of them is heated up by a thermocouple that can be set by the operator. The last one is the head of extrusion, here generally the temperature is set at a lower value in order for the polymer to maintain a viscous behaviour and not be too brittle during the cooling as filament, exiting from a curved junction. Two fans cool it down, while the operator put it inside a wheel that pull it and it becomes a filament. Then the operator must perform the spooling, so insert the filament inside a hole and then inside the spool. When the filament is pulled enough the spool can rotate autonomously. There is also an optical sensor that read the real diameter of the filament and show it on the display, the standard measure is 1.75 mm.

Each type of filament was extruded once, pelletized with a scissor in pellets long around 7 mm and extruded again, to increase the homogeneity of the final product.

Five different filaments were produced:

- Pure PLA
- PLA with the compatibilizer (PLA-C, 90:10)
- PLA, compatibilizer and filler (PLA-C-F, 80:10:10, 85:5:10, 88:2:10)

The settings for the extrusion changed for each of them, for the PLA and the PLA-C the temperatures were 160-180-175-160 °C, for each part of the instrument starting from the head of extrusion, while the speed of the screw was 4 rpm and the fan speed was 40%. For the PLA-C-F the temperatures were 170-175-170-165°C, the speed of the screw was 4 rpm and the fan speed was 40%.

5.2.2. 3D printing

In order to check the mechanical and thermal properties of the materials produced with the extruder and with the FDM technology, some samples were printed with the 3D printer Mustang M400 (Vepram, Italy) represented in *figure 43*. It was used the nozzle with the diameter of 0.4 mm.

The printer is based on different parts:

- the bed, on which there will be the deposition of the fused filament and the creation of the final object. Below the bed there are some thermocouples that heat it up if it's necessary. An alignment of it is always necessary.
- the nozzle, that can be changed depending on the diameter required. Through it there will be the passage of the fused polymer. It will move along some guides that allow it to reach each position on the bed. It is heated up by a thermocouple.
- the chamber of extrusion, inside which the filament changes its physical state and becomes viscous. It is heated up by a thermocouple.
- the wire feeder, that must be set depending on the hardness of the material. If the diameter of the filament is not constant, the operator must change the setting, otherwise the extrusion will be stopped.

Figure 43 3D printer Mustang M400

The printing parameters were:

- For the PLA: extrusion temperature of 205°C, heatbed of 60 °C, multiplicator of the extrusion of 0.92, speed of the nozzle of 20 mm/s. The filament diameter was set at 1.75 mm
- For the PLA-C: extrusion temperature of 225°C, heatbed of 70°C, multiplicator of the extrusion of 0.95, speed of the nozzle 20 mm/s. The filament diameter was set at 1.65 mm, since it was not as regular as the one of PLA.

Different samples were printed:

- For the tensile test with the dynamometer, samples with a dog bone shape were produced, their measurements followed the law ASTM D638 (Type V);
- For the DMA analysis, samples with a bar shape were produced following the law ASTM D5026, and their measurements were 25 x 4.5 x 2.4 mm;

5.2.3. Characterization

AT-IR

The spectroscopic characterization of all the materials was performed using the spectrophotometer Alpha (Bruker, Germany) in *figure 44* with Attenuated Total Reflectance (ATR), that is a type of measurement in which the samples do not require previous preparation. In this instrument there is a diamond crystal from which will exit the radiation, above that we will put the sample (simply deposing it if it is liquid or pressing it in order to avoid air voids if it is solid). First we have to clean the crystal with isopropanol, then measure the background (32 scan) and finally putting the sample on the crystal and starting the final measure (64 scan from 400 cm^{-1} to 4000 cm^{-1} at 4 cm^{-1} for resolution). In this way we were able to see the main functional groups of the materials and provide some information about their chemical composition.

Figure 44 Alpha spectrophotometer with ATR

TGA

Thermo Gravimetric Analysis (TGA) were performed to analyse the thermo-degradative properties of the materials, using the TG 209 Libra (Netzsch, Germany) in *figure 45*. All the analysis were performed in nitrogen atmosphere, with a ramp of 20°C/min from 30°C to 600°C followed by an isotherm at 600°C for 10 minutes. It was used a alumina crucible in which, after the tare, was put the sample and was inserted inside the thermobalance of the instrument.

Figure 45 TG 209 Libra

DSC

The thermal properties of the materials were analysed using the Differential Scanning Calorimetry DSC Q2000 (TA Instrument, USA) represented in *figure 46* linked to the cooling system RCS. The samples where weighted (around 2-4 mg) and put inside a standard aluminium pan. They were inserted in the autosampler of the instrument in which it withdrew them and put inside the analysis cell comparing them to another empty pan of reference. The measurement was performed with a first heating from -40°C to 240°C with a ramp of 20°C/min, followed by a cooling from 240°C to -40°C with a ramp of 20°C/min and last with a second heating from -40°C to 240°C with a ramp of 20°C/min. The final results consider only the second heating.

Figure 46 DSC Q2000

Dynamometer

The mechanical properties were measured with a tensile test performed with the dynamometer Remet TC10, with a load cell of 1 KN. The test was performed with a speed of movement of the crosspiece (so of deformation of the sample) of 2 mm/min. The samples were printed with the 3D printer in a dog bone shape (*figure 47*), following the norm ASTM D638 TYPE V for their measures, both at 0° and at 90°. Each sample was first measured with a digital calibre, in order to normalize with more accuracy the stress and strain measured. We obtained the elastic modulus, the maximum stress at breaking and the percentual deformation at breaking of all the samples.

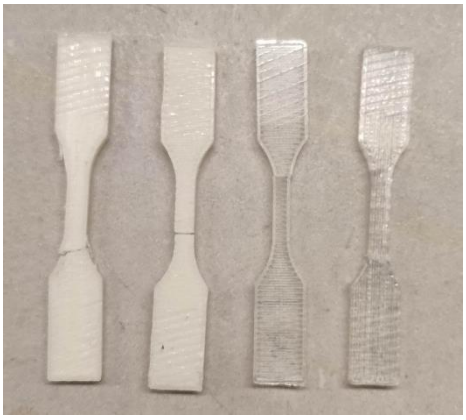

Figure 47 Dog bone samples of PLA-C (first and second samples) and PLA (third and fourth samples) printed along 0° direction (first and third sample) and along 90° direction (second and fourth samples)

NMR

The functionalization rate of the compatibilizer was checked with the acquisition of a ^{1}H-NMR spectra with the instrument Varian Mercury 400 working at 400 MHz. The sample was dissolved in DMSO, with heating.

DMA

The samples were analysed with the dynamo-mechanic analyser Artemis 242E (Netzsch, Germany) in *figure 48*, with the geometry in tension, in which the sample is clamped in two clamps and a stress is applied longitudinally along the specimen. The parameters set for the analysis are resumed in the following *table 11*

Table 11 parameters used for the DMA analysis

Parameter	**Value**
Frequency	1 Hz
$F_{dynamic}$	5.0 N
Proportional factor	1.1
Deformation	50 µm
F_{static} additional	0.1 N

The analysis was performed with heating, from 30°C to 100°C with a ramp of 3°C/min.
The samples were measured with a digital calibre in order to normalize the obtained values inside the software of analysis.

Figure 48 DMA Artemis 242E

6. References

[1] M. Rujnić-Sokele, A. Pilipović, “Challenges and opportunities of biodegradable plastics: A mini review”, Waste Management & Research, 2017

[2] https://tecnopolo.bo.cnr.it

[3] L. Mazzocchetti, “Biopolymers and sustainable polymers”, University of Bologna, 2021, unpublished

[4] C.S.K. Reddy, R. Ghai, Rashmi, V.C. Kalia, “Polyhydroxyalkanoates: an overview”, Bioresource Technology 87 (2003)

[5] A. Mehmood et al., “The current status and market trend of polylactic acid as biopolymer: Awareness and needs for sustainable development”, Materials Today: Proceedings, 2022

[6] S. D. Shetty, N. Shetty, “Investigation of mechanical properties and applications of polylactic acids—a review”, Material research express, 2019

[7] M. C. Zhang, B. Guo, J. Xu, “A review on polymer crystallization theories”, Crystals, 2016

[8] X. Shi et al., “Comparison of precipitated calcium carbonate/polylactic acid and halloysite/polylactic acid nanocomposites”, Journal of Nanomaterials, 2015

[9] S. Farah, D. G. Anderson, R. Langer, “Physical and mechanical properties of PLA, and their functions in widespread applications – A comprehensive review”, Advanced Drug Delivery Reviews, 2016

[10] M. Savioli Lopes, A. L. Jardini, R. Maciel Filho, “Poly (lactic acid) production for tissue engineering applications, 20th International Congress of Chemical and Process Engineering CHISA 2012, 25-29 August 2012, Prague, Czech Republic

[11] M.S. Islam, K.L. Pickering, N.J. Foreman, “Influence of accelerated ageing on the physico-mechanical properties of alkali-treated industrial hemp fibre reinforced poly(lactic acid) (PLA) composites”, Polymer degradation and stability, 2009

[12] A. K. Mohanty, M. Misara, G. Hinrichsen, “biofibres, biodegradable polymers and Biocomposites: An overview”, Macromolecular Materials and Engineering, 2000

[13] R. Hsissou et al., “Polymer composite materials: A comprehensive review”, Composite structures, 2021

[14] F. Avilés et al., “Carbon nanotube-reinforced polymers”, pp.83-115, 2018

[15] K. N. Bharath, S. Basavarajappa, “Applications of biocomposite materials based on natural fibers from renewable resources: a review”, Science and engineering of composite materials, 2015

[16] D. Carlson, L. Nie, R. Narayan, P. Dubois, “Maleation of Polylactide (PLA) by reactive extrusion”, Journal of applied polymer science, 1999

[17] https://www.acs.org

[18] A. Marais et al., “Toward an alternative compatibilizer for PLA/cellulose composites: Grafting of xyloglucan with PLA”, Carbohydrate polymers, 2012

[19] L. Robeson, Historical Perspective of Advances in the Science and Technology of Polymer Blends”, Polymers, 2014

[20] Z. W. Abdullah, Y. Dong, I. J. Davies, S. Barbhuiya, “PVA, PVA blends, and their nanocomposites for biodegradable packaging application”, Polymer-plastic technology and engineering, 2017

[21] A. Morone, M. Apte, R.A. Pandey, “Levulinic acid production from renewable waste resources: Bottlenecks, potential remedies, advancements and applications”, Renewable and sustainable energy reviews, 2014

[22] A. S. M. Bashir, Y. Manusamy, “Recent Developments in Biocomposites Reinforced with Natural Biofillers from Food Waste”, Polymer-plastics technology and engineering, 2014

[23] P. Toro, R. Quijada, M. Yazdani-Pedram, J. L. Ariascd, “Eggshell, a new bio-filler for polypropylene composites”, Material letters, 2007

[24] A. A. Hussein, A. A. Sultan, Q. A. Matoq, “Mechanical behaviour of low density polyethylene / shrimp shells composite”. Journal of Basrah researches, 2011

[25] S. Chonsakorn, S. Srivorradatpaisan, R. Mongkholrattanasit, “Effects of different extraction methods on some properties of water hyacinth fiber”, Journal of natural fibers, 2019

[26] D. Jaiswal et al., “Review on extraction, characterization, surface treatment and thermal degradation analysis of new cellulosic fibers as sustainable reinforcement in polymer composites”, Current research in green and sustainable chemistry, 2022

[27] J. Siroky et al., “Alkali treatment of cellulose II fibres and effect on dye sorption”, Carbohydrate polymers, 2010

[28] A. Awal, M. Rana, M. Sain, “Thermorheological and mechanical properties of cellulose reinforced PLA bio-composites”, Mechanics of materials, 2014

[29] Y. Xiong et al., “Intelligent additive manufacturing and design state of the art and future perspectives”, Additive manufacturing, 2022

[30] M. Bhuvanesh Kumar, P. Sathiya, “Methods and materials for additive manufacturing: A critical review on advancements and challenges”, Thin-Walled Struct., 2021.

[31] W. L. Ng et al., “Vat polymerization-based bioprinting—process, materials, applications and regulatory challenges”, Biofabrication, 2020.

[32] A. Guerrero-de-Mier, M.M. Espinosa, M. Domínguez, “Bricking: a new slicing method to reduce warping”, the Manufacturing Engineering Society International Conference (MESIC), 2015

[33] J. J. ijdam, D. Agarwal, B. S. Schon, “An experimental assessment of filament-extrusion models used in slicer software for 3D food-printing applications”, Journal of food engineering, 2022

[33] A. Dey, N. Yodo, “A Systematic Survey of FDM Process Parameter Optimization and Their Influence on Part Characteristics”, Journal of manufacturing and material processing, 2019

[34] L. Musa et al., “A review on the potential of polylactic acid based thermoplastic elastomer as filament material for fused deposition modelling”, Journal of material research and technology, 2022

[35] L. Fontana et al., “An investigation of the influence of 3d printing parameters on the tensile strength of PLA material”, Materials today: proceedings, 2022

[36] M. M. Hanon, J. Dobos, L. Zsidai, “The influence of 3D printing process parameters on the mechanical performance of PLA polymer and its correlation with hardness”, 10th CIRP Sponsored Conference on Digital Enterprise Technologies (DET 2021) - Digital Technologies as Enablers of Industrial Competitiveness and Sustainability, 2021

[37] S. Bhagia et al., “Critical review of FDM 3D printing of PLA biocomposites filled with biomass resources, characterization, biodegradability, upcycling and opportunities for biorefineries”, Applied materials today, 2021

[38] A. Guevara-Morales et al., “Composite of polylactic acid and microcellulose from kombucha membranes”, E-Polymers, 2020

[39] Y. Tokiwa, B. P. Calabia, “Biodegradability and biodegradation of poly(lactide)”, Applied microbiology and biotechnology, 2006

[40] Geyer R., Jambeck J.R. e Law K.L, “Production, use and fate of all plastic ever made”, Science Advances, 19 July 2017

[41] https://www.plasticportal.eu

[42] https://www.marketsandmarkets.com

[43] Master's degree thesis of Gianluca Vergara “Produzione di un filamento a base di acido polilattico additivato con rinforzo di origine naturale per additive manufacturing”, University of Bologna, A.A. 2017-2018

[44] Master's degree thesis of Marco Capriotti “Utilizzo di scarti agroalimentari nella produzione di biocompositi per additive manufacturing”, University of Bologna, A.A. 2020-2021

[45] https://analyzing-testing.netzsch.com

Acknowledgements

I would like to express my special thanks to my supervisor, prof. Laura Mazzocchetti, and to its special guide that was fundamental in the realisation of this project. The subject of this study was very stimulating, and with her special aid it was possible for me to further increase my interest for it.

I would like to extend my special thanks to my co-supervisors, dr. Paola Natali, for her steady assistance during this study, that was fundamental for me, dr. Niccolò Giani, for its special aid in the first part of the project, and dr. Stefano Scurti, for its special assistance during the part of synthesis and for its great helpfulness.

I would also like to thank all the people who worked in the polymers laboratory in the university of Bologna, I found in each of them a valuable support during all the research.

Finally, I would like to express my heartfelt thanks to my friends and family, since they were present in every success and in every failure, continuing to believe in me, more than I did with myself. What I reached today would not have been possible without them.